Renewable and Sustainable Energy Reviews 47 (2015) 519–539

Contents lists available at ScienceDirect

Renewable and Sustainable Energy Reviews

journal homepage: www.elsevier.com/locate/rser

Review of the applications of microreactors

Xingjun Yao [a,*], Yan Zhang [a], Lingyun Du [a], Junhai Liu [a,*], Jianfeng Yao [b,**]

[a] Shandong Provincial Key Laboratory of Chemical Energy Storage and Novel Cell Technology, School of Chemistry and Chemical Engineering, Liaocheng University, Liaocheng 252059, PR China
[b] Department of Chemical Engineering, Monash University, Clayton, VIC 3800, Australia

ARTICLE INFO

Article history:
Received 11 September 2013
Received in revised form
31 August 2014
Accepted 9 March 2015

Keywords:
Modify
Structured microreactors
Microchannel
Microfluidic
Catalytic film

ABSTRACT

Microreactors offer excellent mass and heat transfer performance for extraction and multiphase reactions. They provide a powerful tool for process intensification and micro scale processing. This paper reviews the structures of microreactors and units, and their applications on the synthesis of nanoparticles, organics, polymers and biosubstances. The structural evolution and properties of the commercialized and lab-made microreactors are introduced in detail. Recent developments of the fabrication, structures and applications of micro-structured reactors are highlighted. The promising direction in science and technology for future microreaction technology is also discussed.

Contents

1. Introduction . . . 519
2. Multiphase microstructured devices to synthesize inorganic and metal nanoparticles . . . 520
   2.1. Synthesis of inorganic nanoparticles . . . 520
   2.2. Preparation of metal nanoparticles . . . 523
   2.3. Controllable monodisperse multiple emulsions . . . 524
3. Synthesis of organic in microstructured reactors . . . 526
   3.1. Microstructured reactors for gas–liquid–solid reaction . . . 526
   3.2. Microstructured reactors for gas–liquid phase reactions . . . 528
   3.3. Microstructured reactors for liquid–liquid phase reactions . . . 530
      3.3.1. Liquid–liquid organic reaction in microreactors . . . 530
      3.3.2. Polymerization reaction in microreactors . . . 535
      3.3.3. Bio-synthesis in micro-structured reactors . . . 536
4. Conclusion . . . 537
Acknowledgments . . . 537
Appendix 1 Abbreviation of microreactors and other . . . 537
References . . . 537

1. Introduction

Micro-synthesis technique in both interdisciplinary engineering and sciences connects physics, chemistry, biology, and engineering arts for various applications. A microfluid segment in microreactor is defined as a minimum unit having microproperties that can be used to improve various unit operations and reactions in microspace. Chemist George Whitesides initially created inexpensive microfluidic devices using poly

* Correspondence to: No. 1 Hunan Road, Liaocheng University, Liaocheng City, Shandong Province, PR China. Tel./fax: +86 6358230056.
** Correspondence to: Room 212, Building 69, Clayton Campus, Monash University, Clayton, VIC 3800, Australia.
E-mail addresses: y_xingjun@163.com (X. Yao), jhliu_01@sina.com (J. Liu), yaojianf@gmail.com (J. Yao).

http://dx.doi.org/10.1016/j.rser.2015.03.078
1364-0321/

dimethylsiloxane (PDMS), and through the microreactor community led by the Institute for Molecular Manufacturing (IMM) in Germany and Yoshida's Microreactor Initiatives in Japan, considerable interest in the microreactor area has been built up. High throughput screening in microanalytical chemistry [1], biological analysis of cells and proteins [2], reaction kinetics and mechanisms studies [3] were the initial uses of microreactors. Microreactors have shown superior heat and mass transfer rates, and the contact time, shape and size of the interface between fluids can be easily and precisely controlled [4]. These attributes make microreactors ideal for fast reactions [5], highly exothermic reactions [6], and even explosive reactions [7,8]. The small volume capacity of microreactors has also allowed the efficient development of more sophisticated continuous flow reactions on increasingly complex molecular targets since they greatly reduce the quantities of materials needed to optimize reaction conditions.

Microreactors are fabricated in a range of materials, including ceramics, polymers, stainless steel, and silicon. The microreaction devices can be classified into two groups: chip-type microreactors and microcapillary devices. Chip-type microreactors offer several advantages including easy control of microfluidics, and integration of many processes into one reaction device. Manufacturing processes of such devices are mainly adaptations from the microelectronics industry. Dry- or wet-etching processes have been used for creating channels on a silicone or glass plates. Glass microreactors offer the benefit of visualizing the reaction progress, but are limited in reactor designs due to the difficulty of creating high aspect ratio structures. Polymer-based materials (e.g. Poly-dimethylsiloxane (PDMS), polymethylmarthacrylate (PMMA), polycarbonate, and Teflon) can be used for preparation of enzyme microreactors because most enzyme reactions have been performed in aqueous solution, especially for bio-analytical use. Stainless steel microreactor networks range from simple systems comprised of T-shape micromixers and narrow tubing to commercial systems with micro-fabricated components [9]. They can be operated at high pressure and temperature. These plates can be processed by photolithography, soft lithography, injection molding, embossing, and micromachining with laser or microdrilling. The LIGA (Lithographie Garbanoforming Abforming) process that combines lithography, electrochemical technology and molding, can also be used for the production of microreactors.

Many efforts have recently been made to prepare microreactors and microseparators, with the aim of achieving better control of the reaction parameters. Micromixers are usually designed to use active micromixing technique, and external energy inputs are acoustic, electrical, thermal, pressure disturbance or integrated microvalves, and pumps [10]. On the other hand, in passive mixing, there is an induced perturbation in the flow in order to enhance mixing, which is accomplished by interdigital multilamellae arrangements, eddy formation, nozzle injection in flows and collision of jets. The most common microstructures designs for passive mixing found are zig-zag microchannels, the incorporation of flow obstacle within the channels, T-, ψ- and Y-flow inlet structures and nozzles [11].

Micro process devices gained interests not only from academic investigations but also from chemical and pharmaceutical industry. Since then, many studies have been devoted to the understanding of the mixing mechanisms and characterizations of microstructured reactors. Five predominant flow regimes in small dimensions are bubbly, Taylar, Taylar-annular, annular, and churn flow [9]. The increasing practice can be deduced from the growing number of research documents, the larger number of participants at microreactor or microfluidic conferences, and the increasing commercialized products of the supplier companies in the field.

We report here the advancements made in the design and modification of microreactor structure over the last ten years and include the improvements in the synthesis of inorganic materials and organic reactions. Some excellent reviews have been published in the area that focused mainly on the reaction/process, the product properties, and the impact on downstream processing [12–18]. This review is organized into the following Section (1) Introduction, (2) Synthesis of Inorganic and metal nanoparticles, (3) Synthesis of organic microstructured reactors, (4) Conclusion.

2. Multiphase microstructured devices to synthesize inorganic and metal nanoparticles

2.1. Synthesis of inorganic nanoparticles

Fine particles are widely used as materials of many types of chemical industry products. Nagasawa and Mae [19] developed a microreactor with an axle dual pipe on the concepts of two immiscible liquids flowing in the inner and outer tubes, and maintained an annular and laminar flow of separated phases to create a micro space by the outer fluid wall as shown in Fig. 1(a). In this method, a nucleation section and a particle growth section are sequentially connected along the flow in the reactor. Mono-modal spherical particles of titania with narrow size distribution are successfully produced without precipitation of particles at the wall, as shown in Fig. 1(b), the particle size is precisely controlled by changing the diameter of the inner tube. The mean particle size is 45 nm for a tube of 307 μm i.d., 84 nm for a tube of 607 μm i.d., and 121 nm for a tube of 877 μm i.d. In this system, nuclei formation and particle growth proceed at the interface of the two fluids as shown in Fig. 1(c). This kind of axle dual pipe microreactor was verified that the arrangement of a middle layer between reactants is an attractive method for controlling particle properties and achieving stable continuous production. However, the microchannel has a risk of clogging by the precipitated particles, depending on such particle synthesis conditions as the microchannel dimensions and the type of processing. The stable continuous production does not cause clogging of a microchannel and gives high throughput as well, which is also important for industrial production. This was conducted by forming the zeolite synthesis hydrogel micro-droplets in a continuous paraffin phase through pumping a silica solution and an alumina solution respectively into two closely packed stainless steel capillaries positioned in the axis of a PTFE outer tube, followed by crystallization in the PTFE tube at 90 °C [20]. This one-step continuous synthesis method can not only avoid product variations from batch to batch, but also decrease the cost for large scale zeolite synthesis as well as versatile production of different types of zeolites. No clogging occurred during experiments conducted for 8 h.

Recently, semiconductor nanoparticles have drawn great attention due to their excellent characteristics. Yen and coworkers [21] reported a continuous-flow microcapillary reactor for the preparation of a series of CdSe nanocrystals. This reactor consists of a miniature convective mixer followed by a heated glass reaction channel (250 μm inside diameter) maintained at a constant temperature (180–320 °C).The Cd and Se precursor solutions are delivered in two separate flows and combine in the mixing chamber before they reach the heated reaction section. The presence of the chamber is necessary because once the Cd and Se precursor solutions meet at room temperature, they slowly forms small CdSe clusters. This cluster formation results in irreproducibility in the sizes of the final NCs (Nanocrystals) produced by the reactor so the Cd and Se precursors are not mixed until just prior to reaching the heated section. In this continuous-flow system, reactions are performed at steady state, making it possible to achieve better control and reproducibility. Further benefits can be realized by scaling down the reactor dimensions to micrometers, thereby reducing the consumption of reagents during the optimization process and improving the

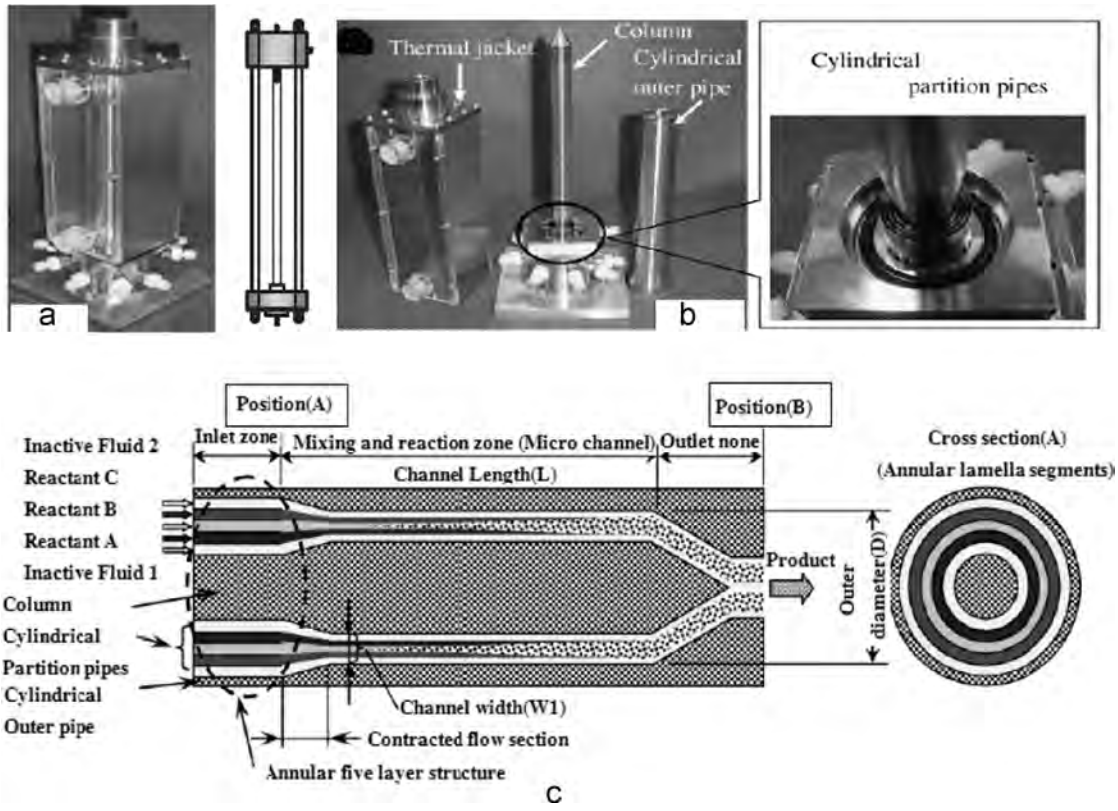

Fig. 1. (a) Overview of the microreactor, (b) internal parts and (c) schematic of flow in the microreactor.
Source: [19].

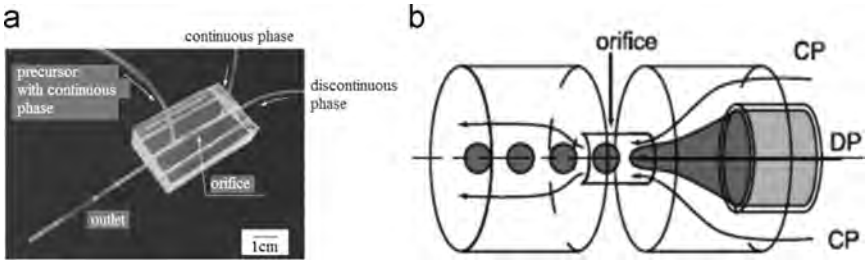

Fig. 2. The fabrication process of AFFD (left) and an axisymettrical flow focusing microchannel (right).
Source: [27].

uniformity of temperature and residence times within the reaction volume.

Wang and coworkers in a microfluidic reactor [22] synthesized highly luminescent CdSe/ZnS nanocrystals. $[(C_2H_5)_2NCSS]_2Zn$ is dissolved in trioctyl phosphine (TOP), mixed with trioctyl phosphine oxide (TOPO), and then injected into the 200 μm, a fused silica, microcapillary reactor to synthesis ZnS. The synthesis of ZnS-capped CdSe in the microcapillary reactor showed an interesting aspect that when the absorption and fluorescence-peak location was compared to the original TOPO-CdSe, the wavelength of the TOPO-CdSe-$[(C_2H_5)_2NCSS]_2Zn$ mixture had slight blue-shifts for short residence times at 240 °C, and then had red-shifts with longer residence time. Possible explanations are the contribution to dissolution of core particles or the formation of composite CdSe/ZnS crystals. This microreactor technology demonstrated advantages in controlling the reaction time both conveniently and accurately. Likely, Chan and coworkers successfully demonstrated droplet formation and flow in a high-temperature microreactor using solvents and conditions that are appropriate for the nanoliter-scale synthesis of CdSe nanocrystals [23]. In a stepped microstructure, controlled streams of octadecene

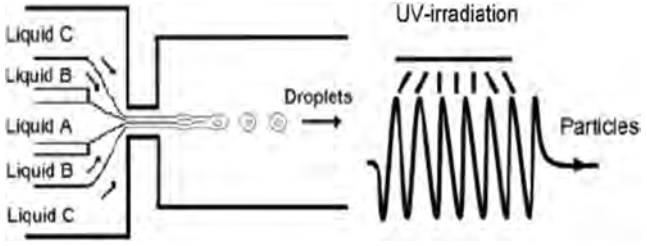

Fig. 3. Schematic of production of droplets in MFFD by laminar co-flow of silicone oil (A), monomer (B), and aqueous (C) phases.
Source: [28].

droplets are generated in perfluorinated polyether at a low viscosity ratio and high capillary number. CdS nanocrystals were synthesized at high temperature in droplet-based microreactors to demonstrate the compatibility of the droplet fluids. The benefits of performing high-temperature nanocrystal synthesis in self-contained nanoliter-scale reaction volumes are discussed in the context of other chemical and biochemical reactions where the physical, temporal, and thermal

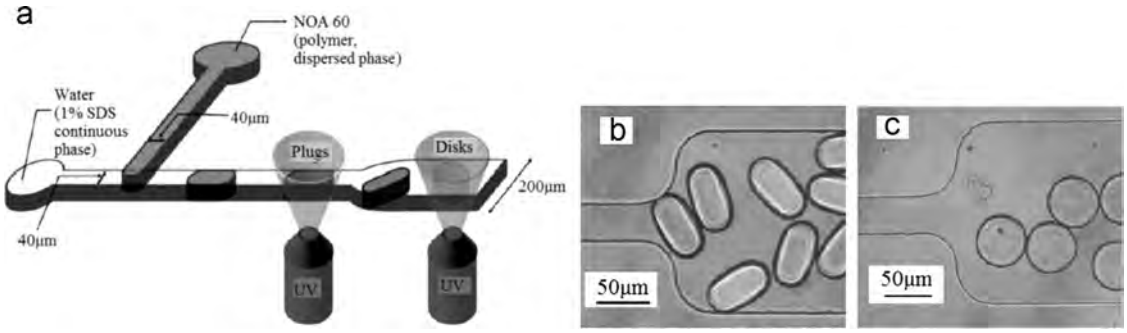

Fig. 4. Microchannel geometry used to create plugs and disks. (a) schematic of channel with plug and disk creation zones marked; (b) polymerized plugs in the 200 μm section of the channel, 38 μm height; and (c) polymerized disks in the 200 μm section of the channel, 16 μm height.
Source: [29].

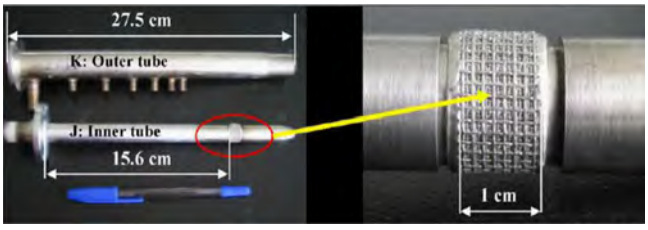

Fig. 5. Schematic diagram for the synthesis of barium sulfate nanoparticles.
Source: [30].

control and isolation of nanoliter-scale reaction volumes are critical elements. These capabilities should be useful in studies of a wide variety of chemical and biochemical reactions. The segmented flow tubular reactor (SFTR) was used for precipitation (calcium carbonate) and crystallization of both inorganic and organic compounds [24]. The laboratory scale SFTR is made up of a micromixer in which the co-reactants are efficiently mixed, and a segmented where the reaction mixture is separated with an immiscible fluid into micro-batch volumes or liquid "bubbles" in a continuous mode. Particle size distributions are narrower, particle shape is more homogeneous, and phase purity is improved.

In Fig. 2, the axisymmetric flow focusing device (AFFD) device was fabricated from a single piece of PDMS [25]. The insulation surrounding an optical fiber (0.25 mm in diameter covered with a 0.75 mm thick layer) was cut with a scalpel and the ends pulled out to expose the fiber. The fiber was embedded in a block after the PDMS had been cured, and the fiber was removed by pulling the fiber out through the end of the PDMS block. Two glass capillaries (0.75 mm outer diameter, 0.5 mm inner diameter) were inserted as an inlet and outlet. The inner aqueous phase is surrounded by the continuous phase and never touches the walls, thus wetting does not occur. Droplets coated with nylon do not contact the walls of the channel in the AFFD, and thus avoid the regions of highest shear. Since the channel is seamless there is no leakage at high flow rates and pressures. This feature allows the production of droplets of liquid encapsulated in nylon-6,6 with a diameter greater than 50 μm. The figure shows the production of droplets in microfluidic flow-focusing device (MFFD) by laminar co-flow of silicone oil (A), monomer (B), and aqueous (C) phases. The orifice has a rectangular shape with width and height of 60 and 200 μm, respectively (left). Schematic of the wavy channel used for photo polymerization of monomers in core–shell droplets (Fig. 3 right). Control over the number of cores per droplet and location of cores in the droplet were achieved [26]. They carried out fast throughput photopolymerization of the monomeric shells and obtained polymer particles with various shapes and morphologies, including spheres, truncated spheres and, hemispheres, and single and multicore capsules in this simple microfluidic flow-focusing device. Xu and coworkers described a MFFD for producing monodisperse solid particles with different sizes (20–1000 mm) and shapes and with narrow dispersity [27,28]. The strategy described has four significant advantages: (1) it offers extensive control over the size and polydispersity of the particles, (2) particles with various shapes can be generated, (3) a range of materials can be applied, including heterogeneous multiphase liquids and suspensions, and (4) useful quantities of particles can be produced.

Microfluidic channels fabricated by pouring polydimethoxysilane (PDMS) on a silicon wafer containing positive-relief channels patterned in SU-8 photoresist is especially necessary to create plugs and disks (Fig. 4) [29]. Fig. 4a shows the channels of two different heights: 38 μm to create plugs and 16 μm to create disks. The micro devices are sealed to glass slides using a PDC-32G plasma sterilizer. Both aqueous and polymer solutions are infused into the channels. The continuous phase is a 1% SDS solution. A UV-sensitive liquid photopolymer that cures when exposed to UV light, is used as the dispersed phase. Monodisperse size and/or morphology can be adjusted by tuning fluid flow properties or the microchannel geometry. Their work showed that microfluidics offers a convenient and finely controllable route to synthesizing nonspherical microparticles with the twin advantages of using soft lithography to design desired geometries and of the ability to exploit fluid mechanics to tune particle morphology.

In a reference describing high-throughput tube-in-tube microchannel (MTMCR) reactor for the large-scale preparation of barium sulfate nanoparticles as depicted in Fig. 5 [30]. The two parts of the reactor are the inner tube and the outer tube. Many micropores are distributed around the wall at the end of the inner tube. The micropore section is composed of several metal meshes. Each mesh is weaved from stainless steel wires of a certain diameter. The meshes are assembled layer by layer with the mesh of larger wire diameter on the surface as a protection layer, followed by pre-calcination, rolling and calcinations at 1280 °C for 3 h to obtain microporous materials. The microporous materials are then rounded and welded to form the annular microporous section of the reactor. The pore size of the microporous materials and the porosity are determined by a bubbling method and then the porosity produced was determined by a comparison of the density of the microporous materials with that of steel. The dispersed solution is forced to flow from the inner tube through the micropores into the annular chamber to mix with the continuous phase from the outer tube. Inner tubes with pore sizes of 5, 10, 20 and 40 μm were employed. The width of the mixing chamber is 750 μm. MTMCR demonstrates unique advantages over conventional microreactors in nanoparticle production due to the high-throughput feature. $BaSO_4$ nanoparticles were also synthesized by precipitation of Na_2SO_4 and $BaCl_2$ at their concentrations close to their saturation concentrations in a commercially available micro mixer, SIMM-V2. The particle size of $BaSO_4$ was dependent on the flow rate at the saturation concentrations, exhibiting a Z-type change with increasing the flow rate. The average particle size of $BaSO_4$ particles could be adjusted by

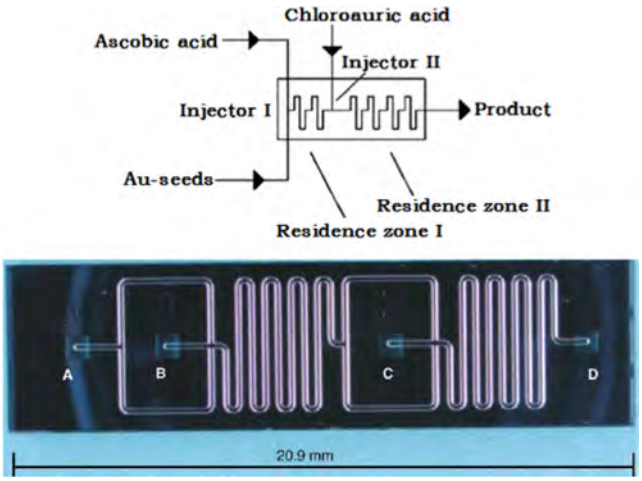

Fig. 6. Photograph of the microchannel reactor for the preparation of Au nanoparticles. A,B,C-inlets, D-outlets.
Source: [34].

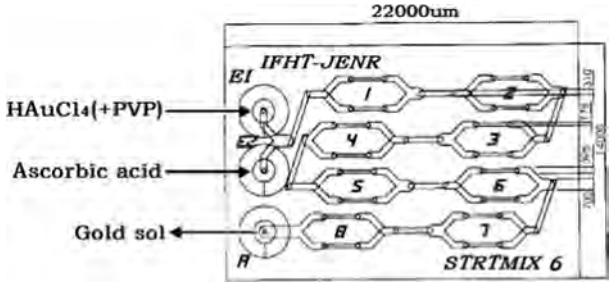

Fig. 7. Schematic drawing of the connectivity of the PIHT (STATMIX 6, area $22 \times 14\ mm^2$).
Source: [35].

decreasing the Na_2SO_4 concentration. The optimized preparation process could produce 2 kg/h of $BaSO_4$ nanoparticles with a mean particle size of 28 nm with a narrow particle size distribution [31]. The particle size of $BaSO_4$ was dependent on the flow rate at the saturation concentrations, exhibiting a constant value first, a decrease afterward, and a constant value again with increasing the flow rate.

2.2. Preparation of metal nanoparticles

The high-precipitation rate and small solubility product of titania can be prepared in the experimental set up [32], namely, the microreactor consists of a transparent glass pipe (external pipe), and a stainless steel pipe (internal pipe). The pipes are coaxially placed, to form a dual pipe structure. The dual pipe structure connects to a microreaction channel that is formed by the external pipe. A thermo jacket surrounding the external pipe controls the temperature. A reactant solution is introduced in the inner and outer pipe areas in the dual-pipe structure of the microreactor. In the microreaction channel, two stratified flows are generated and fine particles are formed in the interface between the two-reactant solutions. The flow generated in the inner pipe is layer A and that generated in the outer pipe is layer B. This reaction operation method has a distinguishing feature. The diameter of the inner laminar flow of annular currents can be controlled by changing the volume flow rate of the inner and outer reactant solutions, without changing the structure of the microreactor, and the temperature gradient and concentration gradient at the interface between the two solutions can be controlled by changing the temperature and concentration of the outer layer solution. Another feature is that the interface between the two reactant solutions in the microreaction channel does not touch the pipe walls, and, hence, technical problems, such as clogging do not arise since fine particles formed do not adhere to the wall. They successfully produced the nanoparticles of 3 nm with a narrow distribution under the low TTIP concentration. Mono-modal spherical particles of titanic were also successfully produced without precipitation of the particles at the wall in the axle dual pipe [33]. It was found that particle size could be controlled in the range from 40 to 150 nm by only changing the diameter of the inner tube at a low TTIP concentration. The study on the titania-fine particles shown here provides a guideline for designing microreactors to form other kinds of fine particles and yields industrially valuable information.

A continuous flow microreactor was used for the synthesis of metal nanoparticles for their high heat and mass transfer rate over batch reactor and easy control of experimental conditions such as pressure, temperature, residence time and flow rate. The microsystem set-up is designed as in Fig. 6. The microchannels are wet etched in Pyrex glass and covered with a layer of silicon, which is anodic bonded to the glass. The reactor possesses two residence zones and four microfluidic ports (A–D) that are etched into the silicon. The microreactor with a volume 2.3 μL and its components are connected via a flexible PTFE tube (inner diameter: 0.3 mm). Low continuous flow rates in the order of 10 μL/min can be achieved, and larger gold particles of diameters ranging from 12 to 24 nm were firstly prepared in microchannel reactors without blocking the channels [34]. Although, there are difficulties accompanying the handling of heterogeneous systems in microreactors, such as adhesion, transport behavior and particle adsorption. The microreactor was especially made by the staff at IPHT Jena, and embedded in the microsystem environment with the assistance of Moller et al. in the experiments.

In another reference described by Wagner and coworkers, the microreactor possesses eight split and recombination units (Fig. 7) [35], which are designed for an optimal reshaping of the cross-section of stacked fluid column parts. The flow direction is changed from horizontal to vertical and vice versa at branching and reunification points, which facilitates an efficient interdiffusion, i.e., an effective mixing. The reactor is connected to the syringes via flexible PTFE tubing and educt solutions are pumped into the micromixer at total flow rates between 500 and 8000 μL/min. Mixing of the two educt streams is achievement

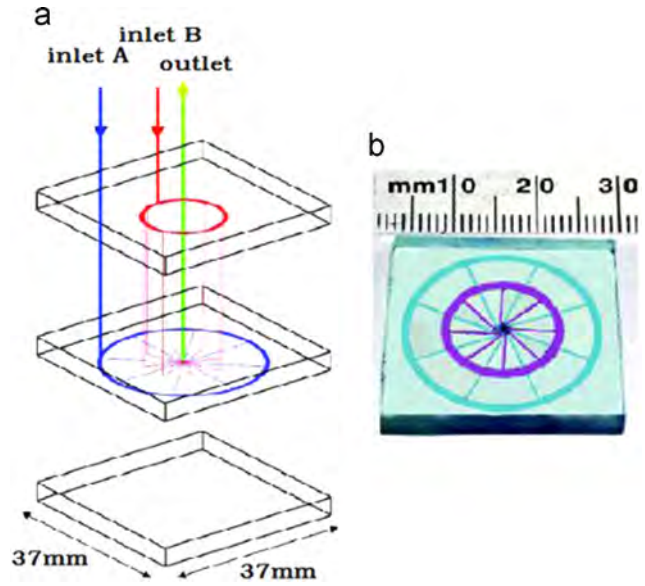

Fig. 8. (a) Schematic of a radial interdigitated mixer (b) Photograph of the fabricated mixer. Microchannels are filled with dye solutions to show different shadings for the different channels [37].
Source: [37].

by inter-diffusion between the manifold split and recombination lamellae of the laminar stream of both solutions, leading to the generation of colloidal gold particles by reduction of $HAuCl_4$. An important issue was the surface treatment of the inner walls of the microreactor, since adhesion of gold particles or their nuclei to these surfaces was a major drawback. They were able to reduce this problem via two alternative approaches. One was the salinization of the reactor, and hence less wetting of these surfaces, resulting in an independence of particle yield from flow rate and leading to no reactor fouling. On the other hand, they worked at an elevated pH, which reduced the deposition due to a net negative charge on the particles and the reactors internal surface, leading to mutual repulsion.

Kohler and coworkers prepared third device for the synthesis of gold nanoparticles. This device was prepared by silicon/glass technology using thin film deposition and micro-lithographic patterning [36]. Holes for fluid interconnections were produced by ultrasound drilling. Microchannels within these chips were produced by isotropic etching in HF-containing solutions by means of a chromium mask. Both half shells were attached to each other by anodic bonding. The mixer chip has a size of 14 mm × 22 mm. The reactor contains three mixing zones, two of them composed of four and one of five micro-fluidic steps for splitting, reshaping and fluidic recombination. There are several completely etched-through silicon channels in each mixing zone. The experimental set-up was based on a 2+1+1 static micromixer to test for the successive addition of reaction components in a micro-continuous flow process. The reactor is well suited for the stepwise mixing of reactant solutions. Flow rates of the single reactants between 1 ml min^{-1} and 50 ml min^{-1} were successfully applied. The typical time consumption of each experiment is in the range of seconds up to half an hour. The total reaction volumes of each experiment were in the range of about 0.2–0.4 ml. The reaction conditions were easily varied by changing the flow rates in the reactant channels.

Monolayer protected gold nanoparticles also have been successfully synthesized using microfluidic reactor technology (Fig. 8) [37]. The devices were based on a radial interdigitated mixer design and function by diffusive mixing between 16 input laminate streams. Each mixing structure consists of 3 substrate layers. In the first two layers, input flows are directed to two circular bus channels which split the flow into 8 identical fluid laminate and deliver reagent streams towards a central mixing chamber. The final layer acts as a cover to enclose the channels and as a guide for input and output capillaries. During mixing, flow streams are alternately brought together radially and mixing is achieved via diffusion. The 16 convergent channels have a width of 150 μm and a depth of 50 μm. Initial results show that the control of the rate of addition of reductant allows fine control of mean particle size. It indicates that lowering the RSH: Au ratio leads to the generation of particles with larger average diameters, the total reaction times for the syntheses are of the order of 4–40 s.

Other cases, likely, Song and coworkers demonstrated that the continuous flow polymeric micro reactor fabricated using SU-8 on a PEEK substrate can be used for wet chemical synthesis of nanoparticles. Pd nanoparticles synthesized using these microreactors were found to be nearly monodisperse in comparison with those obtained from the conventional batch process [38]. Cu nanoparticles formed from microfluidic devices were smaller (8.9 nm vs. 22.5 nm) with narrower size distribution, as well as more stable to oxidation [39]. Cobalt nanoparticles with three different crystal structures, face-centered cubic (FCC), hexagonal closed-packed (HCP), and J-cobalt, were generated from a Y-type mixer and microchannel devices [40]. They have developed a phase-controlled synthesis of cobalt nanoparticles using a polymeric microfluidic reactor through variation of experimental conditions such as flow rates, growth time, and quenching procedure. In Table 1 [40–47], CdS, CdSe, TiO_2, Colloidal Si nanoparticle were synthesized in microchannel; A comparison of these metal nanoparticle like Ni, Ag, Ceria, Curcumin, Au, Pt nanoparticle in microstructured reactor, like caterpillar mixer [49], X, Y, T shape micromixer [51–53,58], rectangular micromixer [54].

2.3. Controllable monodisperse multiple emulsions

In the microstructured reactors, clogging of the microchannel is an important issue which has to be taken into consideration for preparation of the nanoparticles. One of the solutions to this issue is to create a two-phase segmented flow pattern in microchannels so that the solid products synthesized in an aqueous phase can be kept away from inner wall of the tube by a gas or oil phase [63]. A microfluidic device can form droplets by dispersing a continuous fluidic into a liquid phase. Okushima et al. reported a novel method for preparing mono disperse double emulsions using a two-step method of droplet formation in microchannel networks [64]. For W/O/W emulsion (Fig. 9), the aqueous drops to be enclosed are periodically formed

Table 1
Nanoparticle synthesis in various microreactors.

Mixers type	Flow rate (mL/min)	Residence time(s)	Dimension of the nanoparticle(nm)	Product	Ref
Microchannel	10–300 μL/min	–	–	CdS	[41]
Microchannel	0.1	5–10 min	2.8–4.2	CdSe	[42]
Microchannel	0.25	7–150	2–4.5	CdSe	[43]
Microchannel	1.5–3.0 μL/min	250–500	2.4–2.69	CdSe	[44]
Microchannel	80–200 μL/min	–	< 10	TiO_2	[45]
Microchannel	100 μL/min	2.0–2.7	–	CdSe–ZnS	[46]
Microchannel	2–20 μL/min	108–120	10–1000	Colloidal silica	[47]
Microchannel	40 μL/min	Several minutes	< 370	Colloidal silica	[48]
Herringbone micromixer	0.5–4.5	–	20–50	Lipid nanoparticle	[49]
Caterpillar mixer	8	46.8–234	68	Nickel chloride	[50]
Micromixer	35 ml/h	750	88	Silica nanoparticle	[51]
Y shape	2	28.8	3–7	Ag nanoparticle	[52]
Microchannel	0.08	< 60	7.4	Ag nanoparticle	[53]
T-mixer	2–20		15	Ceria nanoparticles.	[54]
Membrane dispersion microreactor	4.0	60 min	7	ZnO Nanoparticle	[55]
Impact-jet micromixer	89–196	6.5–8.5	100	Methacrylic nanoparticles	[56]
Glass microreactor	0.05–1.45	< 120	10–50	Au-nanoparticles	[57]
Split and recombined micromixer	–	2–20	500 μm	SeCd	[58]
X-type micromixer	0.4	5 min	< 1.7	Platinum nanoparticles	[59]
Capillary channel	25	15–30 min	530 mm	ZnO/TiO_2	[60]
Slit interdigital microstructured mixer	163.8	> 30 min	50–80	Silica nanoparticles	[61]
Ceramic microreactor	8.5	–	10 μ m	TiN nanoparticles	[62]

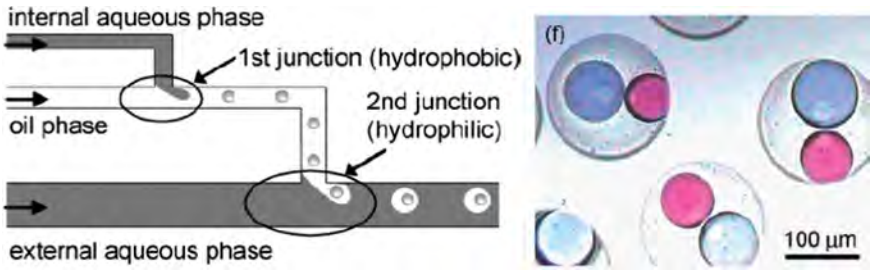

Fig. 9. Schematic (left) of a microfluidic device for creating double emulsions using T-shaped microchannels and (right) red and blue aqueous droplets contained in larger organic droplets.
Source: [64].

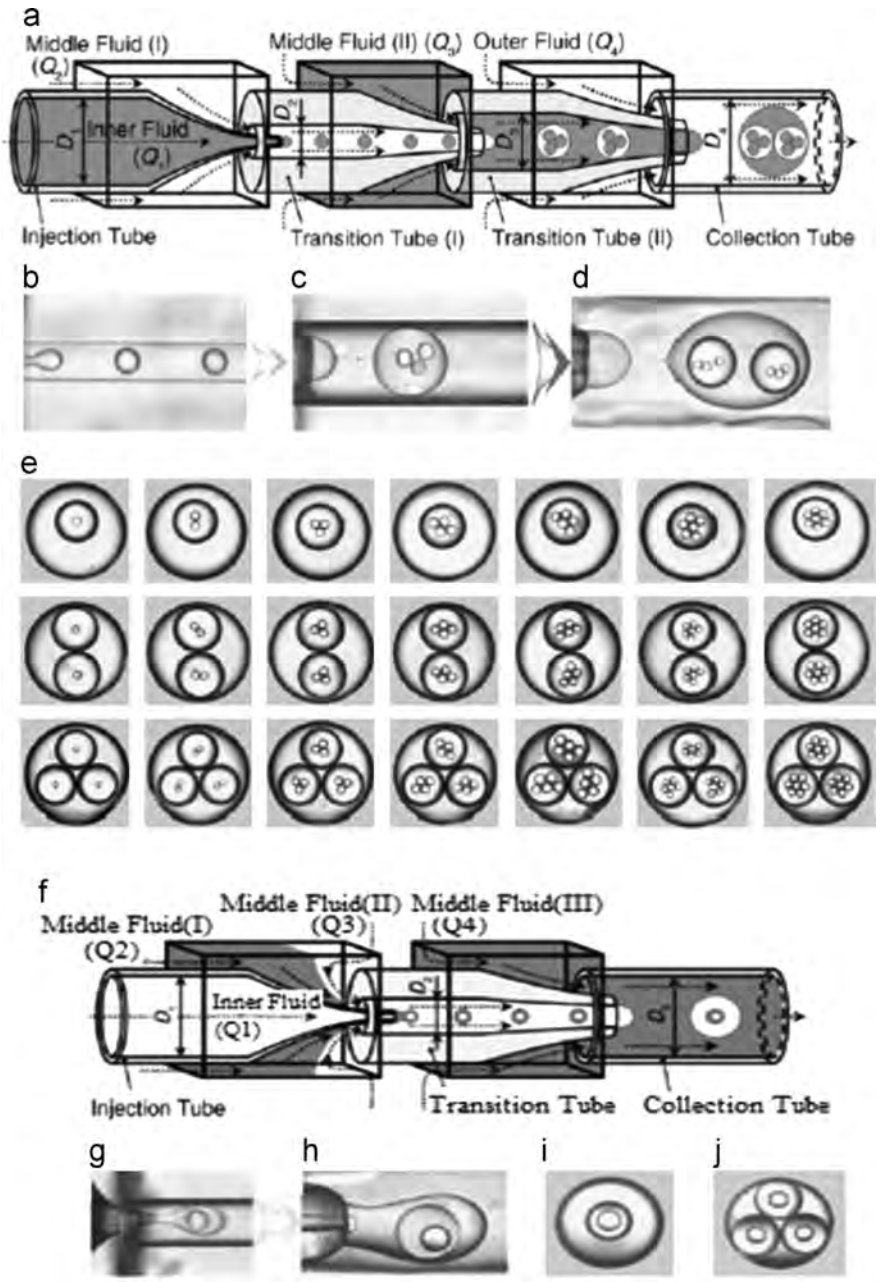

Fig. 10. Generation of highly controlled monodisperse triple emulsions. (a) Schematic diagram of the extended capillary microfluidic device for generating triple emulsions. (b)–(d) High-speed optical micrographs displaying the first (b), second (c), and third (d) emulsification stages. (e) Optical micrographs of triple emulsions that contain a controlled number of inner and middle droplets. (f) Schematic diagram detailing an alternate method for generating triple emulsions where the middle fluid (II) is injected from the entry side of the first square tube, leading to flow-focusing of the first middle fluid into the transition capillary. (g) and (h) High-speed optical micrographs showing the formation of double emulsions in a one-step process in the transition capillary (g) and the subsequent formation of triple emulsions in the collection capillary (h). (i) and (j) Optical micrographs of triple emulsions that contain a different number of double emulsions [67].
Source: [67].

upstream at the hydrophobic T-junction, and then in a continuing series, organic droplets enclosing the aqueous droplets are formed downstream at the hydrophilic T-junction. Droplets of uniform size are formed and their size can be easily varied by changing the flow conditions at the formation points. The number of enclosed drops can be controlled by adjusting the relation between the breakup rates at the two junctions. One-chip module with microfabrication has a smoother connection between the two T-junctions.it is better suited to the precise determination of the number of internal vesicles. These advantages of easy surface modification of one-chip would be most important in the fabrication of integrated multichannels for scaling up the productivity of emulsions. For the two-chip module, strict control of the number of internal drops is difficult because the array of drops to be enclosed that forms in the upstream module tends to be disordered at the connecting area.

Shah and coworkers [65] used capillary-based microfluidic techniques to produce monodisperse poly(N-isopropylacrylamide) gel particles in the size range of 10–1000 μm, and valve-based flow focusing drop formation was developed by Abate et al. to control drop size. In the dripping regime, the drip size is proportional to the continuous phase width of the flow-focus orifice and inversely proportional to the continuous phase flow speed [66]. An advantage of using these PDMS devices is the ease of production. Once a mask is designed, it is easy to produce a large number of devices. Moreover, these devices can be operated in parallel to produce microgels at a much higher rate than can be achieved with a single device.

Furthermore, mixing in the segmented microdroplets is intensified and axial dispersion is eliminated. Chu and coworkers presented a highly scalable microcapillary technique that simultaneously controlled the droplet monodispersity as well as the number and size of the inner droplets [67]. The first emulsification step is accomplished using a coaxial, co-flow geometry. It comprises the injection tube (a cylindrical capillary with a tapered end), which is inserted into the transition tube (a second cylindrical capillary with an inner diameter D2), as shown in Fig. 10. Both cylindrical capillary tubes are centered within a larger square capillary. The alignment is made by matching the outer diameters of the cylindrical tubes to the inner dimensions of the square ones. The opposite end of the transition tube is tapered and inserted into a third, coaxially aligned cylindrical capillary tube, the collection tube, of inner diameter D3. These generate uniform monodisperse multiple emulsions by two emulsification steps. Droplets of the innermost fluid are emulsified in the first stage of the device by coaxial flow of the middle fluid (Fig. 10b). This single emulsion is then emulsified in the second stage through coaxial flow of the outermost fluid, injected in the outer stream through the square capillary (Fig. 10a). In both emulsification steps, droplets immediately form at the exit of the tapered capillary (Fig. 10b and c). The separation of the two emulsification steps allows independent control over each. This is achieved by adjusting the dimensions of the device as well as the inner, middle, and outer fluid flow rates (Q_1, Q_2, and Q_3, respectively). In all their experiments, the variance of the diameters of triple emulsions was less than 1.5%. In addition, the technique can be sequentially scaled to even higher levels of emulsification if desired, for example, quadruple emulsions could be made by adding an additional stage. The coaxial structure of this capillary microfluidic device has the advantage that no surface modification of wettability is necessary, allowing the same device to be used to prepare either water-in-oil-in-water (W/O/W) or the inverse oil-in water-in-oil (O/W/O) multiple emulsions.

3. Synthesis of organic in microstructured reactors

3.1. Microstructured reactors for gas–liquid–solid reaction

An effective, simple micro-structured reactor that can produce such a high interfacial area between different phases is a much-sought-after goal. For example, a microfluidic device for conducting Gas–Liquid–Solid hydrogenation reactions was reported by Kobayashi and coworkers (Fig. 11) [68]. They selected a microchannel reactor having a channel 200 μm in width, 100 μm in depth, and 45 cm in length to synthesis the bonded catalyst. First, amine groups are introduced onto the surface of the glass channel to form 3. Micro-encapsulated (MC) Pd (2), prepared from Pd $(PPh_3)_4$ and copolymer in dichloromethane- t-amyl alcohol, is used as the Pd source. A colloidal solution of the MC Pd 2 is passed through the microchannel to form intermediates, which is heated at 150 °C for 5 h. During the heating, cross-linking of the polymer occurs, and the desired Pd-immobilized microchannel is prepared. Hydrogenation reactions proceed to produce the desired products quantitatively within 2 min for a variety of substrates. The reaction is conducted under continuous flow conditions at ambient temperature by introducing a tetrahydrofuran (THF) solution as the substrate (0.1 M) through one inlet and introducing H_2 through the other inlet via a mass-flow controller. The space-time yield was 140,000 times higher than that produced by ordinary laboratory flasks. No Pd was detected in the product solutions in most cases. The microchannel reactors can be reused several times without loss of activity. This approach should lead to high efficiency in other multiphase reactions. Because it is easy to scale up the reaction by using a number of chips in parallel with shared flow, this system can easily and quickly provide the desired products in the required volumes, as well as in pure form at the point of use without the need for any treatment such as isolation or purification. Such an approach lessens reagent consumption and the time and space needed for synthesis. Document [3] reported polysiloxane immobilized chiral V-salen catalysts which can be coated on silica and glass surfaces. The enantioselectivity of the chosen sulfoxidation reactions was relatively low, allowing us to study the influence of the spacer length of the ligands on the initial reaction rates, conversions and enantioselectivities. The here presented concept can be easily transferred to other catalytic reactions and aid in the screening of a large variety of substrate libraries and to study reaction kinetics using minute amounts of reactants in miniaturized systems. This is of great interest in interdisciplinary research fields such as chemical engineering to design reactions at a miniaturized level.

A titanic-modified microchannel chip (TMC) was fabricated to carry out efficient photo-catalytic synthesis of L-pipecolinic acid from L-lysine [69]. Fig. 12 shows that the TMC was composed of two Pyrex glass substrates (0.7 mm thick). The branched microchannels are fabricated by photolithography-wet etching techniques (770 μm width, 3.5 μm depth). A TiO_2 thin film is prepared on another substrate with a sol–gel method from titanium tetranbutoxide (Kanto) ethanol solution as the starting material. The two substrates are thermally bonded at 650 °C for 4 h in order to obtain the film (300 nm in thickness) composed of approximately 100 nm diameter TiO_2 particles. The TiO_2 particles appear to be an anatase structure known from SEM images and XRD analysis. The most important advantage of the present TMC is applicability to the potential-controlled photocatalytic reactions with high conversion rate, a removal process for the catalyst is unnecessary in the reaction sequence, the product can be separated from the catalyst by the flow, which can improve the selectivity of the product. However, as mentioned above, the reaction efficiency is not high enough due to its small specific interface area. Thus, information on potential-controlled photocatalytic reactions, particularly organic synthetic reactions, is limited.

Chen and coworkers of the Dalian Institute of Chemical Physic reported wall coated catalysts in a microchannel reactor for methanol oxidation reforming [70]. In order to prepare the catalysts for methanol oxidation reforming, the washing-coating layer of CuZnAl is prepared by the sol–gel technique, and then the active layer is coated on it by solution-coating technique with emulsion colloid containing Pd–ZnO particles. Catalysts developed showed highly

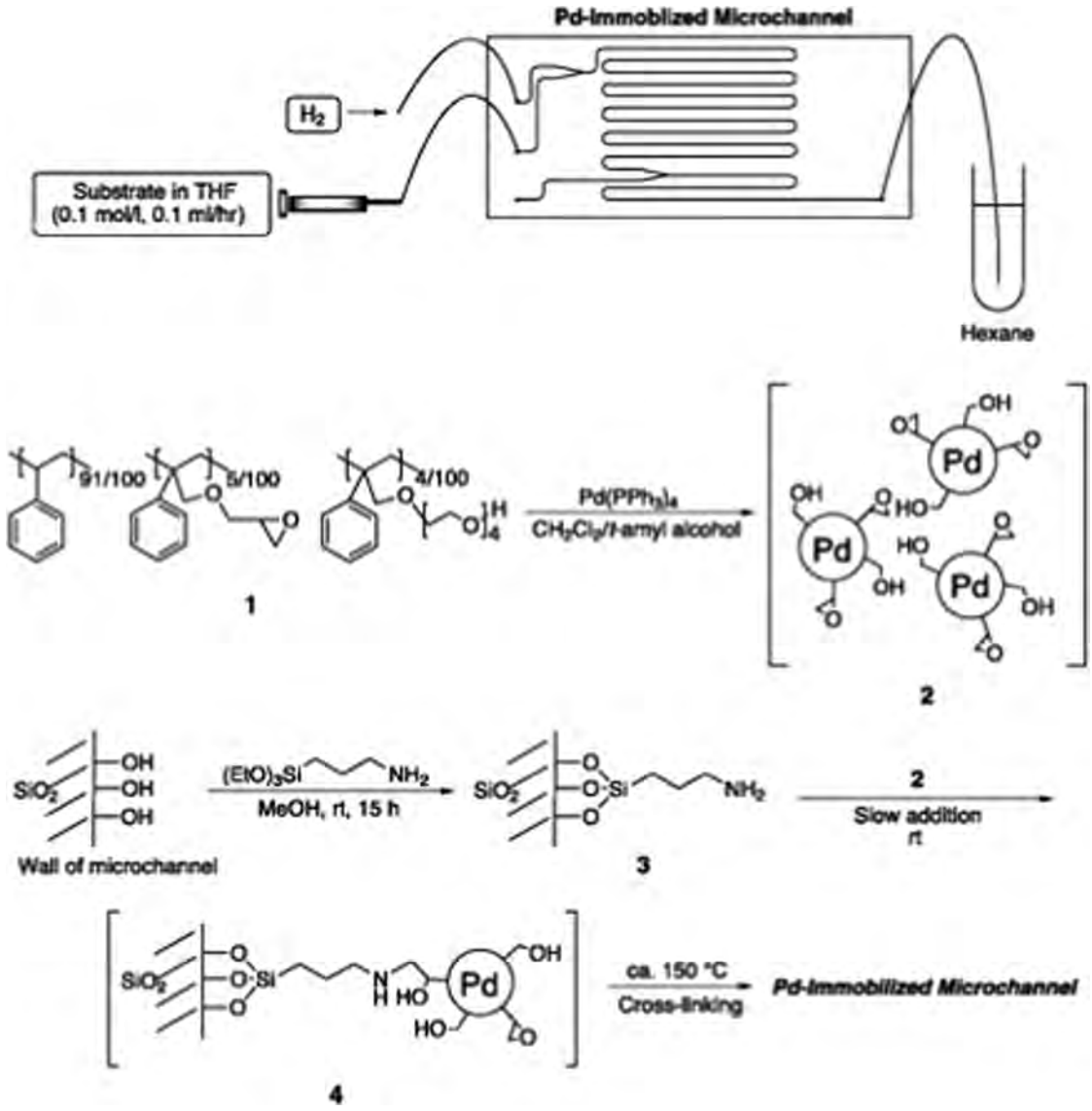

Fig. 11. Experimental hydrogenation system using a microreactor and immobilization of the Pd catalyst.
Source: [68].

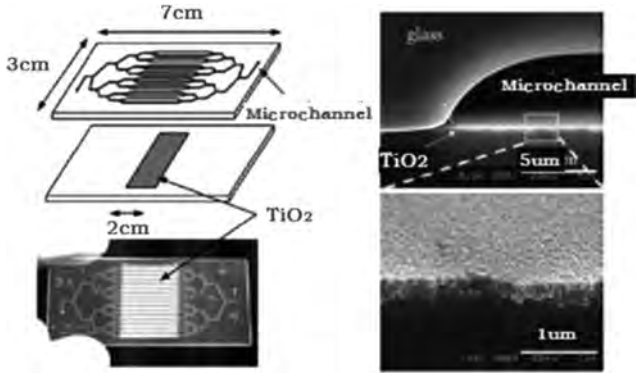

Fig. 12. TiO_2 modified microchannel chip and cross-sectional SEM of the channel.
Source: [69].

activity as indicated by high methanol conversions at high space velocity, while the active layer of Pd–Zn exhibited somewhat easy peel off. This implied that the technique of sol–gel for Cu–Zn–Al wash-coating layer was an effective method for preparing catalysts in stainless steel microchannel plates, however way of solution-coating for Pd–Zn particles should be improved further.

Abdallah et al. reported a continuous micro-structured reactor equipped with a perforated membrane for the gas–liquid–solid asymmetric hydrogenation of ethylpyruvate on a $Pt/\gamma\text{-}Al_2O_3$ catalyst modified with chiral inductors under high hydrogen pressure [71]. The best enantio selectivity (63%) of the eight chiral inductors was obtained with cinchonidine. The very low reaction volume (100 μL) allows for a very short operating time of 1 min. The facility to change various parameters and operating conditions (temperature, residence time, substrate and modifier concentrations, solvents, etc.) without the cumbersome filtration of the catalyst is a real practical advantage. The results have allowed proposing that enantioselectivity can be strongly decreased by selective deactivation. Furthermore, the first quantitative data on the adsorption isotherm of the very popular cinchonidine chiral modifier are presented.

Kolb et al. reported a number of selective oxidation reactions that were carried out in micro-channel reactors [72]. The stable catalyst formulation techniques, tailored for micro-channels, were developed for the preferential oxidation as a gas purification step in the framework of fuel processing. Advance catalysts involving combinations of noble metals, zeolites and other oxide supports permit CO reduction

down to the ppm-level. Micro-combustion can be carried out on a catalyst in which case it is predominantly a heterogeneous reaction involving surface reactions. In catalytic combustion, noble metals like platinum(Pt), rhodium(Rh) and palladium (Pd) supported on to the microcombustor wall using special deposition and drying methods [73].

As described above, titania-modified microchannel chips exhibited a good photocatalytic performance [69]. Zeolite- and ceramic-modified microreactors would also study that have better thermal and chemical stability. Zampieri and coworkers presented a novel zeolite-ceramic composite microreactor with bimodal pores, that was obtained by coating the cell walls of microcellular polymer-derived ceramic foams with a thin, binder-free layer of MFI-type zeolite(silicalite-1 and ZSM-1) [74]. Ceramic foams, which have low thermal expansion coefficients and high thermal, mechanical, and chemical stability, can provide enhanced mass and heat transfer and a low pressure drop when compared to zeolite pellets used in fixed-bed reactors. The composite morphology affects mechanical stability and cell interconnectivity. Takahashi and coworkers [75] prepared a capillary column microreactor with a Cu/SiO_2 layer for catalytic reaction and proved its efficiency by constructing a pulse reaction system using a catalyst column jointed to a column with pure silica gel layer for gas separation. The CuO/SiO_2 column is heated at appropriate reaction temperature whereas the pure silica gel column is held at ambient temperature. After CuO has been reduced to Cu with H_2 flow at 573 K to the Cu/SiO_2 column, the temperature is decreased at prescribed temperatures. Propene pulse is injected into the Cu/SiO_2 column with H_2 as the carrier gas, and the mixed gas of propene and propane is separated in the pure silica separation column. The results elucidate that the silica gel layer on the inner surface of capillary can be a support for metal nanoparticles. Its activity will be designed by simply extending the length of the reaction column, which is favorable for a reaction where high selectivity is only achieved at low reaction temperature with low reaction rate. The capillary reactor is expected to be applied not only for portable use but also for highly designed reaction systems. Cui and coworkers [76] used nano-magnetic particles as a multifunctional microreactor for deep desulfurization. The sulfur level can be lowered from 487 ppm to less than 0.8 ppm under optimal conditions. The main components MSN of nano-magnetic particle are synthesized by the micro-emulsion method. MSN has an average diameter of less than 20 nm, and the magnetic nanoparticles are densely entrapped within the SiO_2 shell. In addition, the surface Si–OH groups can easily react with siloxane coupling agents to provide an ideal anchorage for subsequent formation of a phase-transfer catalysis layer with an ordered structure.

3.2. *Microstructured reactors for gas–liquid phase reactions*

In this section, micro-fabricated reactor for direct gas–liquid phase reactions was described. This device utilizes a multitude of thin falling films that move by gravity for typical residence times of up to about one minute. Its unique properties are the specific interfacial area of 20,000 m^2/m^3 and good temperature control by an integrated heat exchanger. Such high mass and heat transfer was achieved by performing direct fluorination of toluene with elemental fluorine in this device [77–79].This so far uncontrollable and highly explosive reaction could be managed under safe conditions and with control over the reaction mechanism. Via an electro-philic pathway, Lob and coworkers [77] achieved a yield of 20% of o-and p-mono-fluorinated isomers. The single/tri-channel thin-film micro reactor (Fig. 13) has a three-plate structure. The first is a thin frame for screw mounting and providing an opening for visual inspection of the single micro-channel section. The second serves as the top plate for shielding the micro-channel section and comprising the fluid connections. This plate has also functions as a seal and is transparent to allow viewing of the flow patterns in the single micro-channel. The third is the bottom polished plate, which a metal block is bearing the micro-channel. The liquid is fed at one end of the micro-channel and runs through the single micro-channel for passage to adapt to the temperature. Then the gas stream is introduced in the moving liquid via a second port in the rectangular flow guidance. The micro heat transfer module is comprised of a stack of microstructured platelets which are bonded and heated by external sources, e.g. by placing it in an oven or by resistance heating. The single parallel flows are all in the same direction on the different levels provided by the platelets. Distribution and collection zones are connected to inlet and outlet connectors. The micro heat transfer module is used to quickly heat up gas e.g. to the reaction temperature. They also described other micro reactor systems for halogenation reactions, such as the Microbubble column (MBC) which was used for the dispersion of gas in a liquid stream (Fig. 14). It is a gas/liquid contacting device for very rapid reactions, typically in the order of one second and less. The central parts of the MBC are the micro mixing unit and the micro-channel plate. The mixing unit is comprised of an interdigital feed structure with different hydraulic diameters for gas and liquid feeds. Each of the micro-channels on the micro-channel plate is fed by a separate gas and liquid stream. The slug flow pattern, annular or spray-flow patterns can be identified in the MBC. The gas and liquid streams merge in order to be removed from the micro-channel section. The MBC is also comprised of internal cooling via heat conduction from the reaction zone to a mini channel heat exchanger. Enhancements in selectivity, conversion and space–time yields are given.

A dual-micro-channel chip reactor is shown in Fig. 15 [78]. The reaction channels were formed in a silicon wafer by potassium hydroxide etching, silicon oxide was thermally grown over the silicon, thin nickel films were evaporated over the wetted areas to protect them from corrosion, and Pyrex was bonded to the silicon to cap the device. Corrosion-resistant coatings are needed because silicon readily reacts with fluorine at ambient conditions and forms silicon tetra-fluoride. Silicon oxide can then be attacked by the reaction sub-product hydrogen fluoride. However, it was observed that silicon oxide is compatible with mixtures of fluorine in nitrogen (at least up to 25 vol%) at room temperature under scrupulously dry conditions. The

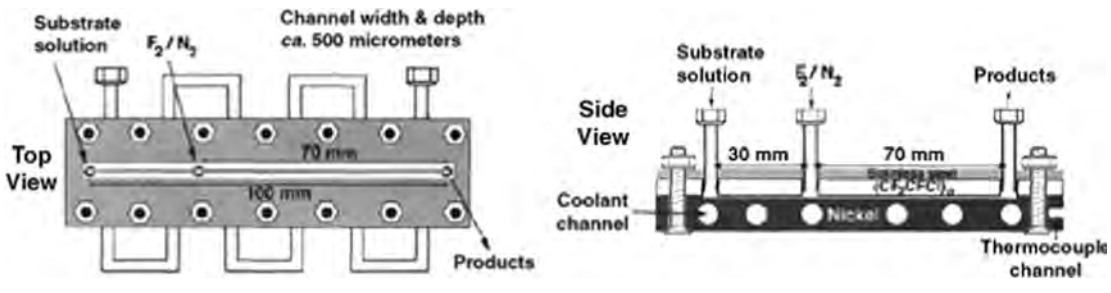

Fig. 13. Schematic illustration of the single-channel micro reactor.
Source: [77].

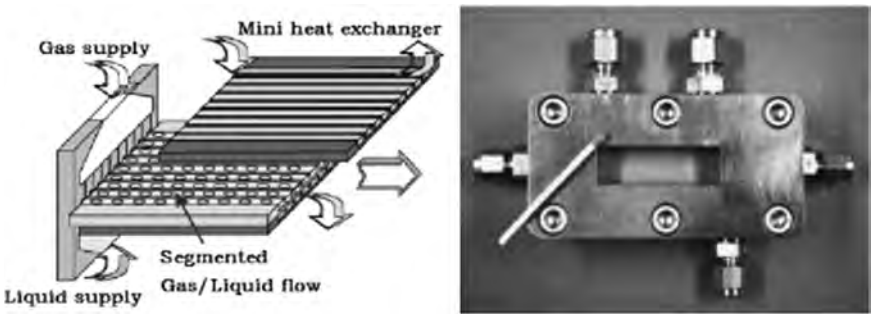

Fig. 14. Schematic illustration of contacting liquid and gaseous reactants in a micro bubble column (left). Micro bubble column (right).
Source: [77].

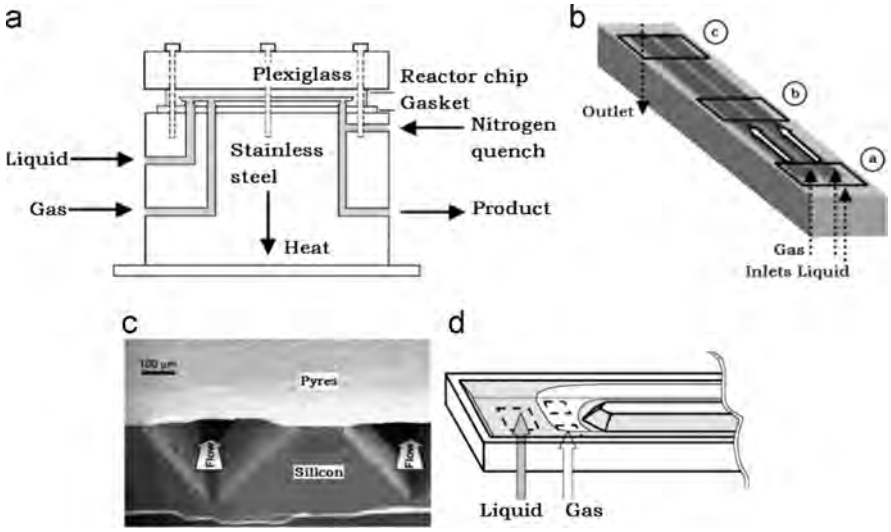

Fig. 15. (A) Packaging scheme of the reactor chip used for carrying out fluorinations. (B) Schematic configuration of the microfabricated reactor. (C) Cross-sectional scanning electron micrograph of the microchannels at the center region. (D) Schematic representation of gas-liquid contacting front in the gas inlet region.
Source: [78].

Table 2
Gas-liquid organics microreactions in different microreactors.

Mixers Type	Flow rate(mL/min)	Residence time(s)	Yield (%)	Product	Ref
Fall film microreactor	3.3 – 17.5	0.5–2.5	82–80(%,conversion)	Octanoic acid	[81]
T-microreactor	–	17.4 min	95	Carboxylic acids	[82]
Dual-channel microreactor	30 μL/min	30 min	72–82	Heck reaction products	[83]
Triple-channel microreactors	–	1 min	49.5–136.5 (STY)	Ascaridole	[84]
Microchannel	15 μL/min	20 min	20	(+)-nootkatone	[85]
			23	Acetaldehyde	
T-junction	0.03–0.15 mL/min	0.01–0.08	15	Acetone	[86]
Mixer			4	Ethyl acetate	
Fabricated microreactor	15.6 mL/min	5–95 min	–	H_2/ Sodium borohydride	[87]
Porous ceramic mesoreactor	0.1–0.3 ml/min	–	71(conversion)	$NaNO_2/H_2$	[88]
Microchannel	0.0075–0.0085 mL/min, 5 mL/min	–	9.9	H_2O_2	[89]

microreactor, schematically represented in Fig. 15B, consists of two reaction channels with a triangular cross section, 435 μm wide, 305 μm deep, and 2 cm long. The hydraulic channel diameter dh (4 times the cross-sectional area divided by the wetted perimeter) is 224 μm, and the volume of the reactor is 2.7 μL. A scanning electron micrograph channel cross-section is shown in Fig. 15C. Microchannels with sloped walls were etched in potassium hydroxide (sidewalls form a 54.7° angle with respect to the plane of the wafer). The advantages offered by microfabrication technology pave a promising path for the commercialization of direct fluorination processes in the near future. A benchtop microreactor array system consisting of a few number of multichannel reactor units operating in parallel is a promising discovery tool for fluorinated aromatics.

Contact of gases with liquid is of a more complex nature. In the example of liquid jet decay, the liquids are combined in the mixing zone and fragmented into droplets. By changing the geometry of the mixing chamber and the wetting properties of the microstructured material used [80]. Table 2 summarizes the available performance data and other key information including residence time, flow rate, yield and products. Based on the data, hydrogenation, Heck reaction, oxygenation reaction etc. can be carried out in various types of microreactor.

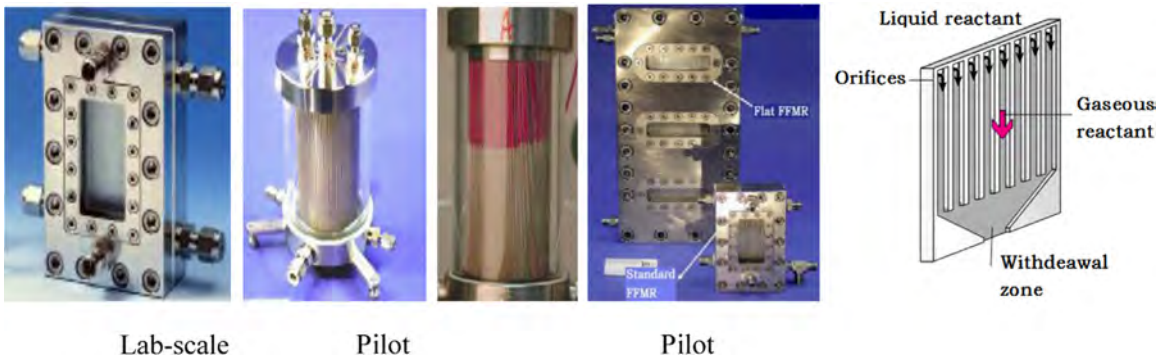

Fig. 16. Falling film microreactor used for gas-liquid mixing process in the lab-scale and pilot (from left to right). The left is the falling film principle in a muti-channel architecture.
Source: [81].

Fig. 17. Degussa's experimental reactor for the pilot operation of a gas-phase reaction.
Source: [93].

The performance of falling-film reactors also can be easy to optimize for very rapid or highly exothermic reactions. They employ thin liquid films that are created by a liquid feed falling under gravitational pull. The liquid film is in contact with a solid support which is usually either a thin wall or stack of pipes. A falling-film microreactor can generate stable films less than 100 μm thick [79,90]. The most critical part of the reactor is the stainless steel plate where the falling film is generated. Microchannels (typically 300 μm wide, 100 μm deep, 78 mm long separated by 100 μm wide walls) are fabricated using electro discharge machining or wet-chemical etching. Supply and withdrawal of liquid are through boreholes which are connected via one large slit to numerous small orifices at the top of the micro channels. The slit acts as a flow restrictor and aids the equipartition of the liquid phase into parallel streams. The entire plate measures 46–89 mm and is housed in a stainless steel enclosure shown in Fig. 16. The structured heat exchange copper plate is inserted into a cavity beneath the falling-film plate for temperature control. The top part of the housing has a view port covered by a thick piece of glass that allows inspection of the entire channel section of the falling-film plate. In this way, the reactor can also be used for photochemical reactions provided the window material is transparent to the wavelength of interest. When both the top and bottom parts of the housing are placed together, a cavity is created above the plate through which the gas flows. In the Kolbe–Schmitt synthesis from Resorcinol [91], the 1/8-in. capillary reactor with a length of 3.9 m and a reaction volume of 9 mL was replaced by a 1 m-long capillary in coil shape having an outer diameter of 1/16 in., an inner diameter of 0.9 mm, and a reaction volume of 0.6 mL. Xie and coworkers prepared the methyl ester sulfonate in a FFMR (HT-07030, IMM, Mainz, Germany). Three microstructured stainless steel plates(64 straight, parallel microchannels, width × thickness: 300 × 100 μm^2; 32 microchannels, 600 × 200 μm^2; 16 microchannels, 1200 × 400 μm^2;) with a size of 89.4 × 46 mm^2 (length × width)were used. The reaction mixture flowed out of the FFMR into a tube. This step was conducted in a tubular reactor with an inner diameter of 3 mm, which was connected right to the outlet of the FFMR [92]. The sulfonation reactions operated with and without liquid overflow did not have obvious difference, suggesting that mass transfer in FFMR was not overwhelming.

There is a pilot plant for heterogeneously catalyzed gas-phase reactions was established in Degussa in Hanau. The core of the plant (which is two stories high) is a microstructured reactor. The aim of this project was to answer key constructive, process, and operational questions, and thereby to demonstrate the feasibility of the direct transfer of the results from the laboratory scale into production on an industrial scale is possible (Fig. 17) [93].

3.3. *Microstructured reactors for liquid–liquid phase reactions*

3.3.1. *Liquid–liquid organic reaction in microreactors*

Microstructured reactors for liquid–liquid phase reactions has been widely used in organic process development, For example, Yube et al. performed an efficient oxidation of aromatics with peroxides under severe conditions using a microreaction system consisting of the standard slit interdigital micromixer as shown in Fig. 18 [94]. The nitration of pyrazoles illustrates several advantages of the same continuous flow reactor for the safe handling of hazardous and

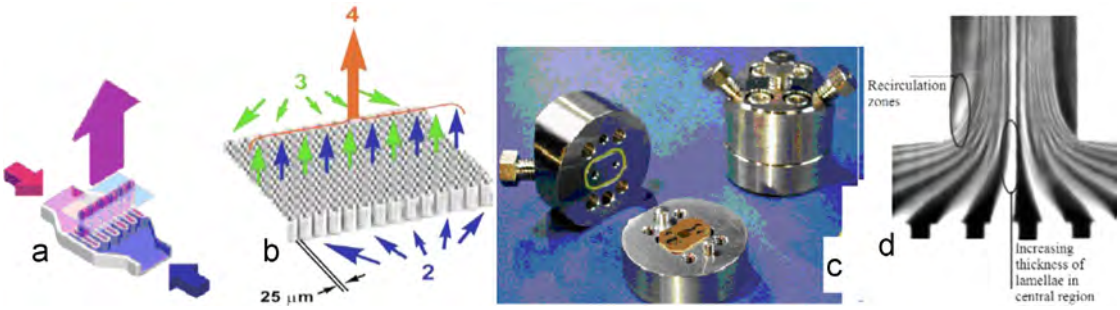

Fig. 18. Standard Slit Interdigital Micro Mixer SSIMM: (a) Interdigital mixing principle (b) multi-lamination with geometric focusing and subsequent volume expansion. Slit Interdigital Micro Mixer V2-SIMM-V2: (c) Individual parts of the SIMM-V2 device (d) SIMM-V2 flow pattern.
Source: [94].

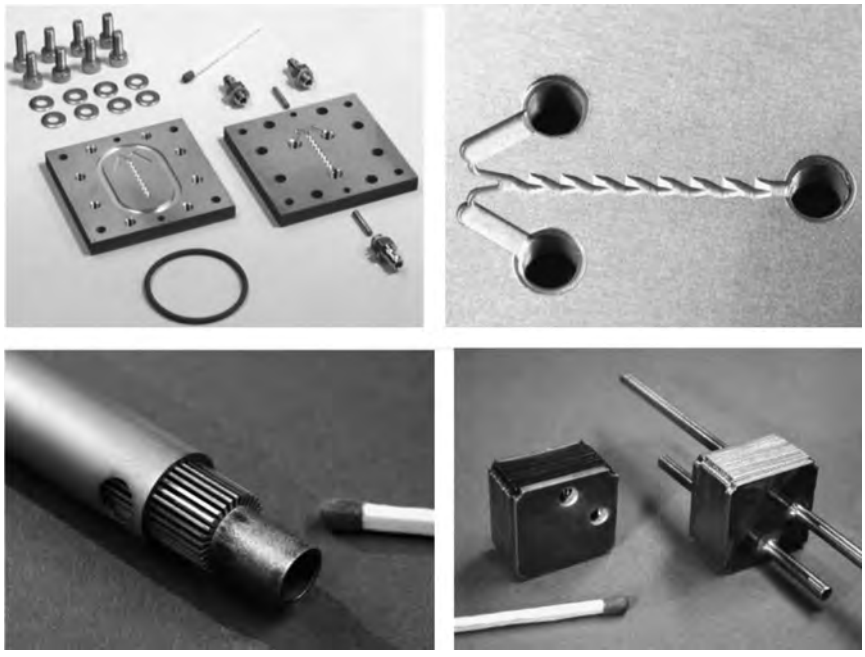

Fig. 19. Microstructured devices used. (Top left) Disassembled caterpillar micromixer CPMM-R1200, mainly showing the two microstructured housing plates. (Top right) Up-down curved ramp-type microstructured channel in the CPMM mixer. (Bottom left) Electrically stirred liquid microstructured preheated "Tube HTMD". (Bottom right): fluidically driven liquid microstructured cooler "CRMH".
Source: [99].

exothermic reactions [6]. Micromixing and precise temperature control make the selectivity of VK3 increased to 50% via the suppression of consecutive side reactions by controlling a short residence time of 30 s at a high temperature of 100 °C. Suga et al. chose Friedel–Crafts type alkylation reactions of aromatic compounds for they envisioned that efficient 1:1 mixing using a micro-scale mixer would facilitate the selective formation of a monoalylation product, and they gained a 96% high yield of product [95]. This micro mixer combines the regular flow pattern created by multi-lamination with geometric focusing and subsequent volume expansion, which speeds up liquid mixing of the multilamellae and leads to jet mixing. The latter process uses eddy-assistance and can utilize turbulent flow. Another version deliberately used multi-lamination/focusing only to avoid jet formation by volume expansion. Due to these advantages, the slit mixer is widely available for processes such as mixing, emulsification, single-phase organic synthesis, and multi-phase reaction. The mixer inlays are high-precision tools fabricated by LIGA (or additionally by ASE) technique guaranteeing high standard of fluid equipartition. As a microreactor, a slit-type interdigital micromixer (SIMM-V2/Ag40) Fig. 18c, IMM Institut for Microtechnology (Mainz GmbH, Germany) was chosen to add secondary amines to α, β-unsaturated carbonyl compounds and nitriles [96]. By using a continuous-flow microstructured reactor rig, the reaction time could be shortened from 96 h (batch) to 13 s (microstructured reactor) at 99% yield without any detectable side products. High production rates are achievable, space-time yields are increased by a factor of up to 650 compared to those of the batch process. Yao et al. present two-step continuous synthesis of tetraethyl thiuram disulfide using microstructured reactors, starting with the formation of N, N-diethyldithiocarbamic acid from carbon disulfide and diethylamine in the first microstructured reactor (SIMM-V2),and the oxidation of N, N- diethyldithiocarbamic acid by hydrogen peroxide in the second one(HPIMM) [97]. These reactions were accelerated by orders of magnitude via ensuring fast mixing and efficient, simultaneous removal of reaction heat under improved thermal control. Kulkarni et al. [98] used SIMM-V2 connected with a reaction tube of 1.3 mm inner diameter, and presented the feasibility of the concept of a miniaturized plant, for analysis of the homogeneously catalyzed equilibrium-limited esterification reaction which was illustrated with butyl acetate synthesis as a model system. This version has the same benefits of mixing as the original standard

version. It improved concerning fluidic connections, e.g. to pumps and tube reactors, as it employs HPLC connectors. Compared to the connectors of the standard version, the HPLC joint to steel tubing improves leak tightness and higher pressure operation can be achieved. The investigations involving the heterogeneous catalytic system yielded good results. Performance of the system was consistently reproducible, and the reactor could be operated continuously for very long time. Similar to the above micromixer and a microfalling-film reactor, an mFBR also has a potential to become an integral component of a microplant.

New microreactor technology of the aqueous Kolbe–Schmitt synthesis was invested by Hessel and coworkers. [99]. This CPMM-Series micromixer has a ramp-like internal microstructure (Fig. 19) within which one channel is alternately directed up and down. This induces, at low Reynolds numbers, a split-and-recombination action which is a sequential multiplication of the number of fluid lamellae, while halving their width. At high Reynolds numbers, circulatory flow presents eddies which lead to interfacial stretching. Diffusion is the major mixing mechanism at low Reynolds numbers, while convection (followed by diffusion) is effective at high Reynolds numbers. Two versions of the CPMM mixer (1.2 mm × 1.2 mm × 19.2 mm) were used in experiments. One with a small channel of 600 μm, CPMM R600, which was supposed to exhibit faster mixing, and one with a large channel of 1200 μm (CPMM R1200). The CPMM devices were manufactured by 3-D micromilling. Compared to a 1-L laboratory flask synthesis, advantages are reduction of reaction time by orders of magnitude (few tens of seconds instead of minutes), increase of space-time yield by orders of magnitude, increase of throughput by a factor of 2 (with option to one magnitude by numbering-up), simple and flexible upgradeable rig, for laboratory and pilot throughputs. Otherwise, the disadvantages of the new microreactor technique are the following: partly unstable plant operation due to pronounced sensitivity to fouling, unreliable resorcinol analysis due to resorcinol deposits and decomposition reactions in the plant, capital and energy expenditure for high temperature and pressure operation.

The Beckmann Rearrangement of Cyclohexanone Oxime to ε-Caprolactam in a microreactor provides a nice example of the effectiveness of microreactors in solving such selectivity problems [100]. The microreactor consists of a low-temperature mixing zone followed by a high- temperature reaction zone (Fig. 20). The large channel has a width of 312 μm and the small channel has a width of 122 μm. The top and bottom sides are interconnected by laser drilled holes with a diameter of 250 μm. The mixing is conducted in a split-and-recombination micromixer and a microchannel at 65 °C, followed immediately by a second microchannel at 100–127 °C to obtain complete conversion. A two-stage technology of low-temperature to induce reaction, and high-temperature to enhance reaction is developed. Under these conditions the formation of microdroplets ranging from 10–25 μm, the residence time of the reactants in the microreactor setup is less than 40 s, and the corresponding molar ratio of oleum to cyclohexanone oxime can be reduced to 0.8 from the industrial value of 1.2, a selectivity of 99% has been achieved. Other highly exothermic organic reactions, including methyl ethyl ketone (MEK) peroxidation was carried out in a microchannel reactor (Fig. 21) [101]. The micromixing unit consists of four plates made of stainless steel. The inlet and outlet plates act as housing, while the inlet plate is also jointly used with the distribution plate to distribute different feeds. The mixing plate has four channels (300 μm width and 40 μm depth) and an aperture (0.6 mm diameter). The outlet plate also has an aperture in the center, which is 2 mm in diameter. The mixing plate is fabricated by chemical etching while the others by precise machining. The inlet tubing and outlet tubing are serpentine stainless-steel pipes of 1 mm inner diameter. Lengths of the inlet and the outlet tubing are 200 and 800 cm, respectively. In this reaction process, all the peroxidation and post-processing steps can be controlled automatically. Demixing or demulsification is to be carried out in microchannels. Neutralization, devolatilization, and dehydration, to increase the flash point, the stability and the appearance of the product also be confined in small channels. With minimum process improvements, many of highly exothermic reactions, reactions carried out at high temperatures, reactions involving unstable intermediates and reactions employing hazardous reagents can be carried out both safely and effectively on microreactors [7,8].

Zigzag micro-channel reactors were fabricated and used for continuous alkali-catalyzed biodiesel synthesis. Micro-channels were patterned on the stainless steel (316L) by electric spark processing. As shown in Fig. 22, three types of patterned sheets were prepared to construct the reactor. The medium sheet as a zigzag micro-channel on it. The cover sheet has two holes, which act as the flow paths. The micro-channels all rectangular with the same length of 1.07 m. Surfaces of all sheets of three types were polished to a roughness of 2lm followed by cleaning in acetone prior to diffusion bonding. The bonding process was carried out at 1000 °C for duration of 3 h under 10 MPa pressure in a vacuum of 2×10^{-3} Pausing a diffusion welding furnace. After the diffusion bonding, the samples cooled to room temperature and no heat treatment was applied. Two ferrules fitting were then bonded on the outlet and inlet of the cover sheet as flow joint [102]. The experimental results show that smaller channel size (hydraulic diameter of 240 μm), more turns (350/1.07 m) and the intensification of overall volumetric mass transfer by passive mixing at the microscale are favorable for the formation of smaller droplets, which results in higher efficiency of biodiesel synthesis.

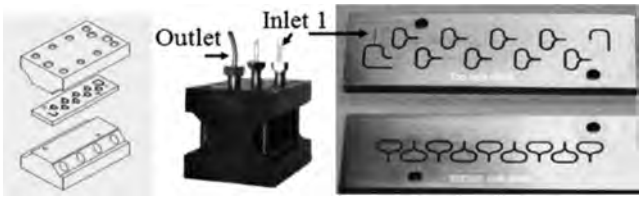

Fig. 20. The split-and-recombination micromixer with a protective coating of diamond-like-carbon (DIARCr). The left picture shows a schematic view of the microstructured plate, with a bottom and top cover. The middle picture shows the assembled mixer. The right picture shows the top and bottom sides of the laser drilled microstructured plate.
Source: [100].

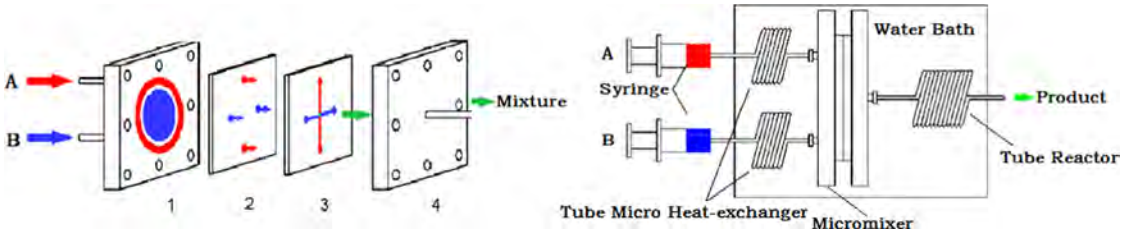

Fig. 21. Configuration of the micromixing unit. (1) Inlet plate; (2) distributing plate; (3) mixing plate; (4) outlet plate.
Source: [101].

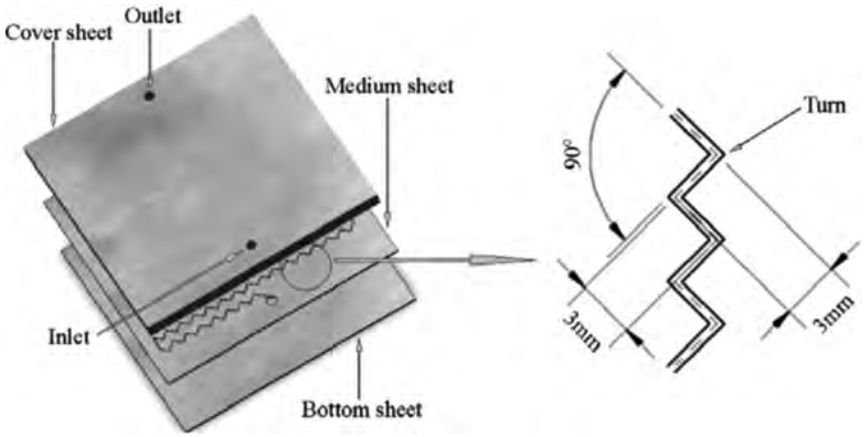

Fig. 22. Reprehensive configuration of a zigzag micro-channel reactor.
Source: [102].

Table 3
Result of liquid-liquid organic synthesis with different microreactors.

Mixers type	Flow rate(ml/min)	Residence time(s)	Yield (%)	Product	Ref
IMM-V2	0.1 mL/h	10 min	91	[BMIm][PF6]	[105]
T-micromixer	1.5 mL/min	12.6	72	tricyclic sulfonamides	[106]
Flow through microreactor	10–20 μL/min	37 min	45.1	DASB	[107]
Flow injection microreactor	1.56 μL/min	20 min	97	Aromatic amidoximes	[108]
Labtrix S1 microreactor	0.1–25 μL/min	-7.5 s-50 min	90–97	Aromatic amidoximes	[109]
Packed-bed microreactor	0.05–5	0.09–9.4	99.9	Butyl butyrate	[110]

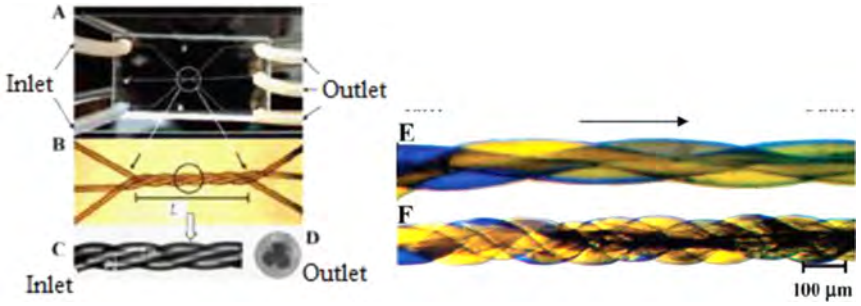

Fig. 23. Schematic of mixing experiment in helical microchannel Triple helical microchannel with controlled mixing length L and the helix angle θ are embedded in block of PDMS. Two differently colored liquid streams are pumped into the microchannel, and three in a typical channel.(E,F) Optical images of the side view of microchannels depict progressive mixing of liquids. (E) Obtained for a channel with helix angle and mixing length. microchannel. Three or more nylon monofilaments are twisted to a desired degree to achieve a particular twisting angle and axial length.
Source: [110].

Continuous production of biodiesel from high acid value oils in microstructured reactor by acid-catalyzed reactions, they developed a two-step process for fast acid-catalyzed biodiesel production from high acid value oil in a microstructured reactor, which was assembled with an SIMM-V2 micromixer connected with a 0.6 mm i.d. stainless steel capillary [103]. In the two-step process, the acid vale of the acid oil was decreased to 1.1 mg KOH/g with methanol to FFA molar ratio of 30 and a sulfuric acid concentration of 3 wt% at 100 °C for 7 min in the first step, and the final FAME yield reached 99.5% after the second step with a methanol to TG molar ratio of 20 and a sulfutic acid concentration of 3 wt% at 120 °C for 5 min. Microchannel reactor was also used for the fast synthesis of acetic acid esters, including methyl acetate, ethyl acetate, n-propyl acetate and n-butyl acetate. Yields of acetic acid ester reached 74.0, 70.1, 97.2 and 92.2% respectively; the residence time was of 14.7 min [104]. It is conclude that decreasing the inner diameter of the microchannel reactor can significantly increase the yield of esters. The reaction temperature near to the lowest boiling point of the components could result in the highest yields of the esters. Fukuyama and coworkers describe an Sonogashira coupling reaction of aryl iodides with terminal acetylenes using IMM mixer-V2, it proceeds efficiently in an ionic liquid [BMIm][PF_6] [105]. Table 3 also summarizes processes on drug synthesis [106], radio synthesis [107], organo-lithium reactions [108] in different types of micromixer.

Enhancing mixing is of great concern in many microfluidics applications, in particular when conducting liquid-phase chemical reactions on the microscale. Verma and coworkers presented novel three-dimensional (3D) microfluidic channel systems that were generated monolithically in poly-dimethylsiloxane (PDMS) using twisted nylon threads as a template [110]. The channels were generated in the form of helices with cross sections consisting of three or more branches, the orientation of which changed along the length of the channel. Such design led to inherent asymmetry of the channel cross-section compared with conventional circular and rectangular microchannels, and was systematically altered by varying the number of the branches.

Fig. 24. Photographs of the mixer array: mixing parts made by an electroforming process in the frame of the LIGA process, single mixing unit and mixer array (top image); single and assembled pieces of the mixer array, mixer and housing consisting of top and bottom plates (bottom image).
Source: [111].

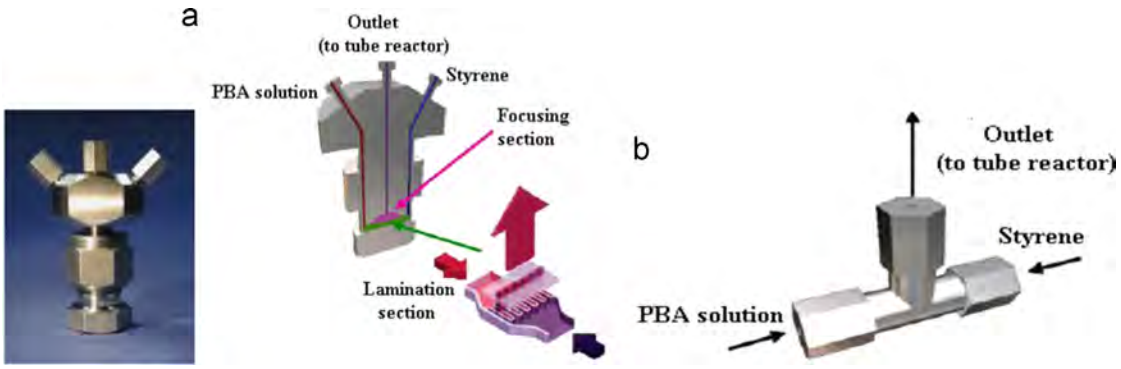

Fig. 25. Microfludic devices considered: (a) High pressure interdigital multilamination micromixer and (b) T-junction.
Source: [114].

Experiments of helix angle and the mixing length of the microchannel on mixing of two different liquids showed that the helical mixer facilitated a strong chaotic flow even at a low Reynolds number, which enhanced the mixing efficiency. Fig. 23 depicts the process of preparing the template for generating the microchannels. Several strands (three to seven) of nylon monofilaments of diameter 50 μm are fixed at equal angular spacing to two parallel rigid cylinders, one of which is rotated relative to the other. The spacing between the disks and the extent of revolution is adjusted to twist the filaments to a desired twisting angle and axial length, which are monitored using a microscope fitted with a camera. The twisted structure is then heated at 100 °C for an hour to form a permanent template which is embedded inside a block of PDMS (Sylgard 184 elastomer). The cross-linked block is immersed in a suitable solvent (e.g., chloroform and triethylamine), which swells the polymer by 25–30% by length but did not affect the nylon thread. The filaments of the thread are then withdrawn by gently pulling them out of the swollen block, leaving behind a helical channel. The PDMS block is unswollen by slow evaporation of the solvent. Fig. 23 shows the cross section of a typical microchannel, which consists of three branches corresponding to a template, generated using three monofilaments.

The mixing quality of a single mixing unit and mixer arrays (Fig. 24) having various designs were characterized by Erfeld et al. [111]. The housing of the micromixers was fabricated of stainless steel by conventional precision engineering applying drilling, micromilling, or microelectron discharge machining (μ-EDM) techniques. For the mixer array the outlet ring (mixing zone) was fabricated by micromilling, while for the single mixing unit (μ-EDM) using a rotating electrode was applied (60 μm width of mixing zone). Mechanical sealing was performed between the top plate and the mixer array (LIGA device) by tight contact of polished surfaces and, against the environment, by an O-ring surrounding the mixing element. The housing was designed to withstand pressures up to 30 bar and was equipped with connectors for the fluids. Geometric focusing was used to reduce lamellae width and to speed up mixing. In the super focus mixer, liquid mixing time is reduced to about 10 ms, as determined by iron-rhodanide reaction imaging. Hardt and coworkers studied the flow patterns and mixing properties of micromixing devices described above by computational fluid dynamics (CFD) and semianalytical methods [112]. Both the model and experiments suggested that geometric focusing of a large number of liquid streams is a powerful micromixing principle. An asymmetrical T-shaped micromixer with replaceable channels was used to comparatively investigate the micromixing performance in various micromixing configurations by the Villermaux/Dushman method and CFD simulation [113]. The results showed that both the convergence region and mixing channel contributed considerably to the mixing. Adaption for one-dimension scale-up in the vertical (or horizontal) direction strategy needs lower mechanical energy dissipation per mass at higher operational capacity. The Re can be used as a fundamental criterion for an asymmetrical T-shaped micromixer in adjusting the width of the mixing channel according to the operational capacity. A microreactor was designed using the approximate pressure drop model [1]. Flow uniformity was validated by CFD analysis and μ-PIV measurements. It demonstrates that there are multiple jet-like flows in the inlet of the reaction chamber; however, flow above the gold layer became uniform due to viscous diffusion. The velocity profiles from experiment agree well with those from the CFD results. Therefore, the fluorescent antibody technique verified that the performance of antibody-antigen binding above the gold film nano-layer in the microreactor was excellent based on flow uniformity. The developed design method can be extended to various microscale biochemical reactors, including SPR chips.

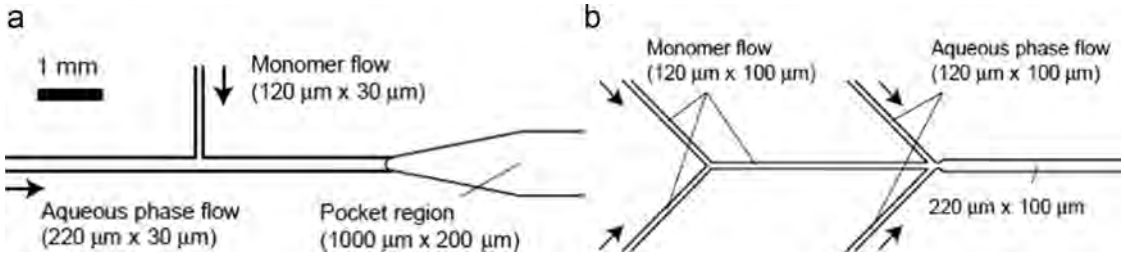

Fig. 26. Schematic representation of channel used for droplet formation (a) T-shaped and (b) Y-shaped channel with two co-flowing channels.
Source: [116].

Table 4
The polymer synthesis in Microfluidic Reaction System.

Mixers type	Flow rate (mL/min)	Residence time(s)	Conversion(%)	Product	Ref
Microchannel	100 μL/h	–	92	2-Hydroxypropyl methacrylate	[118]
Microchannel	240 μL/h	188	69	PEO-b-PHPMA	[119]
T-shape micromixer	0.2–1.0	4.0 min	89.6 (yield%)	BA, BMA MMA, VBz, St	[120]
HPIMM and LH_2	9.7–12.3	150–190 min	91	poly(n-butyl acrylate)-block-poly(styrene)	[121]
Microchannel	5	< 1 min	> 95	Alkene – enone polymer	[122]
Slit-interdigital mixer	0.5	1–5 min	100	Stylene	[123]
Microchannel	1	25 min	100	Styrene	[124]
Microchannel	5 μL/min	4	99(%,yield)	4-$MeOC_6H_4$	[125]
Microchannel	0.06–1.8	4 min	88(%,yield)	Benzyl methacryalte	[126]
Microchannel	65 μL/s.	-120	90	Polycaprolactone	[127]
Microfluidic reactor,	50–200	10 s-several minutes	100	Polytriproplylene glycol diacrylate acrylic acid	[128]
Microfluidic reactor	1.5–12 mL/h	60	100	Polyglycidyl methacrylate ethylene glycol dimethacrylate	[129]
Microchannel	1.95,3.12	2.92–4.38	-99	Polystyrenes-poly(alkyl methacrylates)	[130]

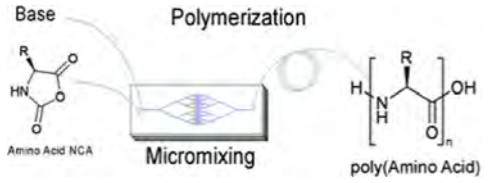

Fig. 27. Microreaction system used for the polymerization of amino acid NCAs.
Source: [129].

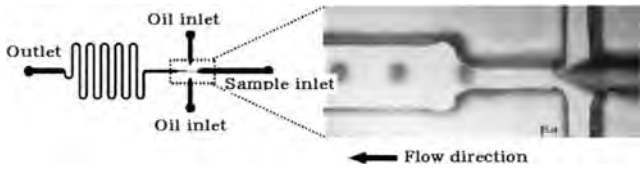

Fig. 28. Schematic drawing of Na-alginate emulsion generator in a cross-junction microchannel.
Source: [131].

3.3.2. *Polymerization reaction in microreactors*

Application of microreaction technology for polymer synthesis has been performed by utilizing a combination of micromixing and reaction parts. The synthesis of poly (n-butyl acrylate)-block-poly(styrene) copolymers by nitroxide-mediated radical polymerization (NMRP) in two serial continuous microtube reactors were performed [114]. The microtube reactors coupled with a multi-lamination micromixer give the narrowest molecular weight distributions, which imply that the control of the copolymerization reaction is improved. Micromixer (HPIMM) came from the IMM Company (Mainz, Germany) and a basic 1/16 in. T-junction (TJ) from Swagelok (Paris, France). The HPIMM laminates both inlet flows (PBA solution+styrene) into 15 lamellae of 20 μm thickness for each flow. These lamellae are arranged in staggered rows and confined in the half-moon shaped focusing section (Fig. 25a). With this micromixer the contact area between the two fluids is greatly increased by the multilamination (ML) of each flow as compared to the TJ micromixer which can be considered as a bi-lamination mixer (BL) with two streams of 450 μm width. The improved control over the polymerization reaction is very important for the synthesis of poly(n-butyl acrylate)-block-polystyrene copolymers due to the highest exothermic monomer gets benefits from the advantages both of the microtube reactor and the microstructured micromixer.

In other exothermic cases, surprisingly narrow molecular weight distributions have been obtained, microtechnological reaction devices demonstrating the promising potential for the tailoring of polymer structures [13]. For example, a microflow system consisting of several microtube reactors can be used at industrial scales under retention of precise temperature and molecular weight distribution control [115]. A pilot plant consisting of a T-shaped micromixer (i.d.=250 μm) and a type-2 shell and tube numbering-up reactor was constructed. Polymerization of methyl methacrylate (MMA) was carried out in the microtubes. The inner diameters of the microtubes in the second, third, and fourth shells were 500, 500, and 1000 μm. Plunger pumps were used for introducing the monomer (MMA, neat, 9.4 mol/L) from a stainless steel tank at the flow rate of 30 or 55 mL/h and for introducing an initiator solution (AIBN in toluene, 0.05 or 0.09 mol/L) from a stainless steel tank at the flow rate of 30 or 55 mL/h. The reaction temperature was automatically controlled by circulating hot oil in the shells, and the cooling temperature was controlled by circulating water in the shells. Obtaining the data with the continuous operation can be speaks well of the potentiality of microchemical plants in the polymer industry.

Nishisako and coworkers also used a simple quartz glass T-junction microchannel (Fig. 26) for synthesizing monodisperse particles of diameters 30–120 m by changing flow rate [116]. They showed a further function by preparing hemispherically colored droplets and microspheres that were subsequently cured. The particle size was reliably chosen in the range of 30–120 μm by controlling flow conditions. Cationic, amionic and free radical

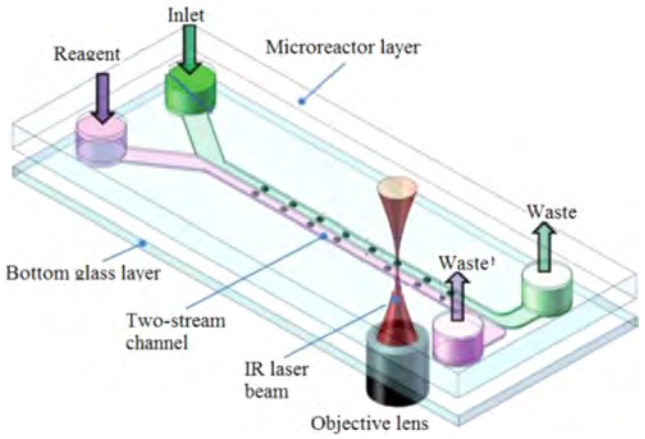

Fig. 29. Schematic configuration of the optical tweezers that direct two stream laminar flow synthesizers with a simplified straight channel and open-end bead confinement features.
Source: [133].

polymerization are three types of polymerization (summarized as Table 4) that have benefited from the microreactor for the rapid mixing and precise temperature control. These references [117–128] showed abundant material with different molecular weights can be prepared within short times by adjusting the flow ratio of monomer and initiator. Potential lie in kinetically controlled polymerizations due to the very rapid reaction in the micromixing device.

3.3.3. *Bio-synthesis in micro-structured reactors*

In biological studies, microreactors have been widely applied to the biosynthesis and biochemical process. Polymerization of α-amino acid N-carboxyanhydride (NCA) in a microreactor tethering multi-lamination micromixer (Fig. 27) yielded better molecular weight distribution, and the average molecular weight could be controlled by changing the flow rate [129]. The PDMS micromixer was attached to a PTFE microtube (∅=250 μm, 500 cm) and served as a reaction region. This microreaction technology offers several advantages, like, polymer with low Mw/Mn values can be obtained at relatively fast reaction rate in base-initiated polymerization. The microreactor allowed narrow molecular weight distribution even with high concentration of NCA. This leads to increase in product yield per unit time, and could be of great advantage in high-throughput synthesis. However, one of the frequent problems encountered when using the microreactor is nonspecific adsorption of reactants and products, especially polymers, to the wall of the reactor. One improvement is to narrow the molecular weight distribution much more, especially in copolymerizations where control of distribution is more difficult. Similarly, Kessler performed the fast polycondensation of trialkoxysilanes in a continuous-flow microreactor to synthesize the defined poly(silsesesquioxane), it achieved a better thermal control and to reduce mass transfer effects [130]. The micromixer (IMM, Mainz, Germany) and tubes (i.d.=0.5 mm, o.d.=1.5 mm) of different lengths(1,3,6,9 or 12 m,respectively) were used to adjust certain residence times. By variation of the residence time molecular weights could be adjusted ranging from 1900 to 11,000 g/mol. Thus, the microreactor setup offers the possibility to synthesize PSSO with adjustable properties.

Huang et al. utilized cross-junction channels to prepare alginate emulsions, and form Ca-alginate microspheres at a $CaCl_2$ outlet reservoir [131]. Gold nanoparticles were encapsulated in alginate spheres to demonstrate the drug delivery capability. The developed microfluidic chip is laid out on a conventional poly methyl methacrylate (PMMA) substrate. This microfluidic chip has three inlet ports, one cross-channel, an observation chamber and one outlet, as shown in Fig. 28. The microfluidic chip is capable of generating relatively uniform micro-droplets and has the advantages of active control of droplet diameter, simple and low cost process, and high throughput. The microfluidic chip is easy to fabricate and set-up, and is easily programmed to generate a large set of ordered Ca-alginate microspheres. The broadened channels (600 mm in width) near the outlet of the cross channel and observation chamber (1 mm in width) are designed for slowing down the flow and enhancing the analysis observation. Liu et al. used a similar flow-focusing channel which comprised of two individual flow-focusing channels and a synthesizing channel is able to produce shape-controlled hydrogel microstructures by a chemical reaction of sodium alginate and $CaCl_2$ [132]. The microparticle morphology and size could be tuned continuously by adjusting the flow parameters in the microfluidic channels. The microfluidic device fabrication process is simple, cost-effective, and flexible in materials, geometries, and scales. Through tuning the microchannel geometry such as the width or the height of the microchannels, the microfluidic device could be applied to produce various kinds of shape-controlled microparticles with wider desired sizes.

An optical tweezers that directed parallel DNA oligonucleotide synthesis methodology is described in which CPG beads act as solid substrates in a two-stream microfluidic reactor [133]. The liquid/liquid interface between these two stream can be maintained with little mixing by running these two stream side-by-side at the same velocity. The selected beads are then captured and transferred using optical tweezers to the corresponding confinement features in the reaction stream, where 5′-DMT is chemically removed and the first nucleotide is coupled. The coupled beads are then capped, oxidized, washed in the reaction stream with sequentially pumped-in reagents and moved back to the inert stream. A simplified microreactor configuration with a straight channel and open-end bead confinement features is shown schematically in Fig. 29. The actual layout used for the experiment that includes side loading channels and more complicated confinements with side openings for bead transport. The patterned top PDMS thick layer has four fluidic ports: two inlets at the Y-shaped ends for reagent and inert chemical delivery and two outlets at the T-shaped ends for waste drainage. The microfluidic reactor is constructed by bonding this PDMS channel layer to a 170 mm thick cover-glass slide, through which the laser beam is transmitted upwards to trap and manipulate beads inside the channel. As a microfluidic-compatible manipulation tool, optical trapping provides significant advantages, including non-contact, rapidly reconfigurable actuation for applications ranging from sorting42 to assembly. These features allow us not only to externally manipulate the beads inside the channel without significantly modifying the microfluidic device itself, but also to open up further possibilities of creating a novel type of versatile, sensitive and multifunctional reconfigurable OBOC bead array on the very same single chip. Moreover, it is feasible to both scale up the diversity by incorporating multiple reactors in a single chip and achieve equivalent total synthesis times as in the production of conventional arrays by implementing well-established, autonomous and automatic computer-controlled high-resolution, high throughput algorithm, programming and synchronization in the optical manipulation system.

In Licklider and Kuhr report [4], they describe the utilization of two proteases (trypsin and pepsin) and a peptidase, carboxypeptidase-Y, in the coupled enzymemodified microreactor-CZE system to perform on-line analysis of protein hydrolysates. Enzymatic microreactors also have been prepared in capillaries and on microfluidic chips by immobilizing trypsin on porous polymer monoliths consisting of 2-vinyl-4,4-dimethylazlactone, ethylene dimethacrylate, and acrylamide or 2-hydroxyethyl methacrylate [134]. The azlactone

functionalities readily react with amine and thiol groups of the enzyme to form stable covalent bonds. The optimized porous properties of the monoliths lead to very low back pressures so that simple mechanical pumping can carry out both the immobilization of the enzyme from its solution and the subsequent analyses of substrate solutions. The good performance of the monolithic microreactor was also demonstrated with the digestion of myoglobin at a fast flow rate of 0.5 mL/min, which gives a residence time of only 11.7 s. The digestion was then characterized using MALDI-TOF MS, and 102 out of 153 possible peptide fragments were identified giving sequence coverage of 67%. The major advantage of this type of microreactor is in scaling up processes which can be achieved by bundling together microcapillaries. Chip-type microreactors have been mainly used for the development of bioanalytical devices.

Self-assembly in micro- and nanofluidic devices have evolved to become indispensable tools to localize and assimilate micro- and nanocomponents into numerous applications [135,136], such as bioelectronics, drug delivery, photonics, novel microelectronic architectures, building blocks for tissue engineering and metamaterials, and nanomedicine.

4. Conclusion

Microreactors have been primarily used as tools for analytical chemistry. Owing to their unique physical and chemical properties, microreactors have exhibited excellent processibility in a range of processes including the synthesis of inorganic, metal nanoparticles and organic, which have been applied in pharmaceutical and chemical engineering in a flexible and controllable manner. Up to now, these microstructured reactors also have been extensively studied as micromixers, and microseparators. Therefore, with small structures that combine different levels of porosities, channels could significantly facilitate diffusion of species. More research efforts is needed to design and fabricate microstructured reactors with optimal channel structure and interconnection, channel size distribution, and channel volume for better yield and selectivity in different systems. Since high performance microreactor structures are readily obtained from glass, ceramic, plastic, silicon or prepolymer, and metal/metal oxide nanoparticles, they have been successfully used in vehicles and aircraft. It would be interesting to incorporate multifunctional nanomaterials into microreactors, which could achieve more functionality and improve their performances in uses such as high-efficiency hydrogenation. Inspired by direct fabrication of microreactors from various materials, it would be worthwhile to devote much effort in the wall-coated microreactor by selecting suitable surfactants and manipulating polymerization conditions [137]. Again, high surface reactivity would enable us to attach functional groups to freshly synthesized microreactors inside nanocomposites or microchannel. The progress of the research into composites-based microreactors has been quite encouraging [138].Successful direct synthesis of microreactors with ordered porous zeolite or ceramic foams with additional functionalities has been achieved. In particular, pilot plant microreactors are valuable when fast reactions are needed, where the outcome will be highly dependent on the mixing quality, and when exploring reactions at high temperature and pressures. Many technical barriers have to be overcome for such connection, parallel control of fluid and reaction conditions, integration, monitoring and critical cost analysis should be conducted, but microreaction technology is sure to evolve and become a new environmentally benign processing technology, which will be widely used in the near future.

Acknowledgments

The authors gratefully acknowledge a support of State Key Laboratory of Materials-Oriented Chemical Engineering, College of Chemistry and Chemical Engineering, Nanjing University of Technology.

Appendix 1. Abbreviation of microreactors and other

Abbreviation name and Specification

AFFD, axisymmetric flow focusing device; block of PDMS ($3 \times 6 \times 1.5$ cm^3)

CPMM, Caterpillar Split-Recombine Micro Mixer; 1.2 mm × 1.2 mm × 19.2 mm, Sus316, 0–100 bar, −20–200 °C, 0.5–250 L/h, group class:-R300, -R600, -R1200, -R2400

FFMR, Falling Film Micro Reactor; 300 μm width,100 μm depth,78 mm long separated by 100 μm wide walls

HPIMM, HiPress Slit Interdigital Micro Mixer; Sus316; 60 MPa; 250 °C; 2 L/h; Width 40 μm × Depth 300 μm

MBC, Micro Bubble Column; gas inlet width 5 μm, liquid inlet width 20 μm

SIMM-V2, Slit Interdigital Micro Mixer-V2; Sus316, 10 MPa, 200 °C, 2 L/h, Width 45 μm × Depth 200 μm

LIGA, Lithographie Garbanoforming Abforming

IMM, Institute for Molecular Manufacturing

PEEK, Polyether Ether Ketone

PTFE, Polytetrafluoroethylene

PMMA, polymethylmarthacrylate

PDMS, polydimethoxysilane.

CFD, computational fluid dynamics

mFBR, miniaturized fixed-bed reactor

SPR, surface plasmon resonance

References

[1] Yi SJ, Park JM, Chang SC, Kim KC. Design and validation of a uniform flow microreactor. J Mech Sci Technol 2014;28:157–66.
[2] Tu ST, Yu X, Luan W, Löwe H. Development of micro chemical, biological and thermal systems in China: a review. Chem Eng J 2010;163:165–79.
[3] Sandel S, Weber SK, Trapp O. Oxidations with bonded salen-catalysts in microcapillaries. Chem Eng Sci 2012;83:171–9.
[4] Licklider L, Kuhr WG. Optimization of online peptide-mapping by capillary zone electrophoresis. Anal Chem 1994;66:4400–7.
[5] Yoshida JI, Nagaki A, Yamada T. Flash chemistry: fast chemical synthesis by using microreactors. Chem – Eur J 2008;14:7450–9.
[6] Pelleter J, Renaud F. Facile, fast and safe process development of nitration and bromination reactions using continuous flow reactors. Org Process Res Dev 2009;13:698–705.
[7] Zhang XN, Stefanick S, Villani FJ. Application of microreactor technology in process development. Org Process Res Dev 2004;8:455–60.
[8] Wootton RCR, Fortt R, de Mello AJ. On-chip generation and reaction of unstable intermediates-monolithic nanoreactors for diazonium chemistry: azo dyes. Lab Chip 2002;2:5–7.
[9] Nagaki A, Takabayashi N, Tomida Y, Yoshida J. Selective monolithiation of dibromobiaryls using microflow systems. Org Lett 2008;10:3937–40.
[10] Nam-Trung N, Zhigang W. Micromixers—a review. J Micromechanics Microengineering 2005;15:R1–16.
[11] Volker H, Holger L, Friedhelm S. Micromixers—a review on passive and active mixing principles. Chem Eng Sci 2005;60:2479–501.
[12] Jahnisch K, Hessel V, Lowe H, Baerns M. Chemistry in microstructured reactors. Angew Chem-Int Ed 2004;43:406–46.
[13] Wilms D, Klos J, Frey H. Microstructured reactors for polymer synthesis: a renaissance of continuous flow processes for tailor-made macromolecules? Macromol Chem Phys 2008;209:343–56.
[14] Mason BP, Price KE, Steinbacher JL, Bogdan AR, McQuade DT. Greener approaches to organic synthesis using microreactor technology. Chem Rev 2007;107:2300–18.
[15] Mae K. Advanced chemical processing using microspace. Chem Eng Sci 2007;62:4842–51.
[16] Erickson D, Li D. Integrated microfluidic devices. Anal Chim Acta 2004;507:11–26.
[17] Neuži P, Giselbrecht S, Länge K, Huang TJ, Manz A. Revisiting lab-on-a-chip technology for drug discovery. Nat Rev Drug Discov 2012;11:620–32.

[18] Moharana MK, Peela NR, Khandekar S, Kunzru D. Distributed hydrogen production from ethanol in a microfuel processor: issues and challenges. Renew Sustain Energy Rev 2011;15:524–33.
[19] Nagasawa H, Mae K. Development of a new microreactor based on annular microsegments for fine particle production. Ind Eng Chem Res 2006;45:2179–86.
[20] Yu L, Pan YC, Wang CQ, Zhang LX. A two-phase segmented microfluidic technique for one-step continuous versatile preparation of zeolites. Chem Eng J 2013;219:78–85.
[21] Yen BKH, Stott NE, Jensen KF, Bawendi MG. A continuous-flow microcapillary reactor for the preparation of a size series of CdSe nanocrystals. Adv Mater 2003;15:1858–62.
[22] Wang HZ, Nakamura H, Uehara M, Yamaguchi Y, Miyazaki M, Maeda H. Highly luminescent CdSe/ZnS nanocrystals synthesized using a single-molecular ZnS source in a microfluidic reactor. Adv Funct Mater 2005;15:603–8.
[23] Chan EM, Alivisatos AP, Mathies RA. High-temperature microfluidic synthesis of CdSe nanocrystals in nanoliter droplets. J Am Chem Soc 2005;127:13854–61.
[24] Jongen N, Donnet M, Bowen P, Lemaître J, Hofmann H, Schenk R, et al. Development of a continuous segmented flow tubular reactor and the scale-out concept-in search of perfect powders. Chem Eng Technol 2003;26:303–5.
[25] Takeuchi S, Garstecki P, Weibel DB, Whitesides GM. An axisymmetric flow-focusing microfluidic device. Adv Mater 2005;17:1067–71.
[26] Nie ZH, Xu SQ, Seo M, Lewis PC, Kumacheva E. Polymer particles with various shapes and morphologies produced in continuous microfluidic reactors. J Am Chem Soc 2005;127:8058–63.
[27] Xu S, Nie Z, Seo M, Lewis P, Kumacheva E, Stone HA, et al. Generation of monodisperse particles by using microfluidics: control over size, shape, and composition. Angew Chem-Int Ed 2005;44:724–8.
[28] Zhang H, Tumarkin E, Peerani R, Nie Z, Sullan RMA, Walker GC, et al. Microfluidic production of biopolymer microcapsules with controlled morphology. J Am Chem Soc 2006;128:12205–10.
[29] Dendukuri D, Tsoi K, Hatton TA, Doyle PS. Controlled synthesis of nonspherical microparticles using microfluidics. Langmuir 2005;21:2113–6.
[30] Wang Q-A, Wang J-X, Li M, Shao L, Chen J-F, Gu L, et al. Large-scale preparation of barium sulfate nanoparticles in a high-throughput tube-in-tube microchannel reactor. Chem Eng J 2009;149:473–8.
[31] Wu H, Wang CQ, Zeng CF, Zhang LX. Preparation of barium sulfate nanoparticles in an interdigital channel configuration micromixer SIMM-V2. Ind Eng Chem Res 2013;52:5313–20.
[32] Nagasawa H, Tsujiuchi T, Maki T, Mae K. Controlling fine particle formation processes using a concentric microreactor. AIChE J 2007;53:196–206.
[33] Takagi M, Maki T, Miyahara M, Mae K. Production of titania nanoparticles by using a new microreactor assembled with same axle dual pipe. Chem Eng J 2004;101:269–76.
[34] Wagner J, Kirner T, Mayer G, Albert J, Khler JM. Generation of metal nanoparticles in a microchannel reactor. Chem Eng J 2004;101:251–60.
[35] Wagner J, Kohler JM. Continuous synthesis of gold nanoparticles in a microreactor. Nano Lett 2005;5:685–91.
[36] Kohler JM, Wagner J, Albert J. Formation of isolated and clustered Au nanoparticles in the presence of polyelectrolyte molecules using a flow-through Si chip reactor. J Mater Chem 2005;15:1924–30.
[37] Shalom D, Wootton RCR, Winkle RF, Cottam BF, Vilar R, deMello AJ, et al. Synthesis of thiol functionalized gold nanoparticles using a continuous flow microfluidic reactor. Mater Lett 2007;61:1146–50.
[38] Song YJ, Kumar C, Hormes J. Synthesis of palladium nanoparticles using a continuous flow polymeric micro reactor. J Nanosci Nanotechnol 2004;4:788–93.
[39] Song Y, Doomes EE, Prindle J, Tittsworth R, Hormes J, Kumar CSSR. Investigations into sulfobetaine-stabilized Cu nanoparticle formation: toward development of a microfluidic synthesis. J Phys Chem B 2005;109:9330–8.
[40] Song YJ, Modrow H, Henry LL, Saw CK, Doomes EE, Palshin V, et al. Microfluidic synthesis of cobalt nanoparticles. Chem Mater 2006;18:2817–27.
[41] Edel JB, Fortt R, deMello JC, deMello AJ. Microfluidic routes to the controlled production of nanoparticles. Chem Commun 2002:1136–7.
[42] Nakamura H, Yamaguchi Y, Miyazaki M, Uehara M, Maeda H, Mulvaney P. Continuous preparation of CdSe nanocrystals by a microreactor. Chem Lett 2002:1072–3.
[43] Nakamura H, Yamaguchi Y, Miyazaki M, Maeda H, Uehara M, Mulvaney P. Preparation of CdSe nanocrystals in a micro-flow-reactor. Chem Commun 2002:2844–5.
[44] Chan EM, Mathies RA, Alivisatos AP. Size-controlled growth of CdSe nanocrystals in microfluidic reactors. Nano Lett 2003;3:199–201.
[45] Wang HZ, Nakamura H, Uehara M, Miyazaki M, Maeda H. Preparation of titania particles utilizing the insoluble phase interface in a microchannel reactor. Chem Commun 2002:1462–3.
[46] Wang HZ, Li XY, Uehara M, Yamaguchi Y, Nakamura H, Miyazaki MP, et al. Continuous synthesis of CdSe–ZnS composite nanoparticles in a microfluidic reactor. Chem Commun 2004:48–9.
[47] Khan SA, Gunther A, Schmidt MA, Jensen KF. Microfluidic synthesis of colloidal silica. Langmuir 2004;20:8604–11.
[48] Gunther A, Khan SA, Thalmann M, Trachsel F, Jensen KF. Transport and reaction in microscale segmented gas–liquid flow. Lab Chip 2004;4:278–86.
[49] Zhigaltsev IV, Belliveau N, Hafez I, A.K.K. Leung, Huft J, Hansen C, et al. Bottom-up design and synthesis of limit size lipid nanoparticle systems with aqueous and triglyceride cores using millisecond microfluidic mixing. Langmuir 2012;28:3633–40.
[50] Zeng CF, Wang CQ, Wang F, Zhang Y, Zhang LX. A novel vapor–liquid segmented flow based on solvent partial vaporization in microstructured reactor for continuous synthesis of nickel nanoparticles. Chem Eng J 2012;204–206:48–53.
[51] Chung CK, Shih TR, Chang CK, Lai CW, Wu BH. Design and experiments of a short-mixing-length baffled microreactor and its application to microfluidic synthesis of nanoparticles. Chem Eng J 2011;168:790–8.
[52] Patil GA, Bari ML, Bhanvase BA, Ganvir V, Mishra S, Sonawane SH. Continuous synthesis of functional silver nanoparticles using microreactor: effect of surfactant and process parameters. Chem Eng Process: Process Intensif 2012;62:69–77.
[53] Xue ZL, Terepka AD, Hong Y. Synthesis of silver nanoparticles in a continuous flow tubular microreactor. Nano Lett 2004;4:2227–32.
[54] Palanisamy B, Paul B. Continuous flow synthesis of ceria nanoparticles using static T-mixers. Chem Eng Sci 2012;78:46–52.
[55] Huang C, Wang YJ, Luo GS. Preparation of highly dispersed and small-sized ZnO nanoparticles in a membrane dispersion microreactor and their photocatalytic degradation. Ind Eng Chem Res 2013;52:5683–90.
[56] Bally F, Serra CA, Brochon C, Anton N, Vandamme T, Hadziioannou G. A continuous-flow polymerization microprocess with online GPC and inline polymer recovery by micromixer-assisted nanoprecipitation. Macromol React Eng 2011;5:542–7.
[57] Pacławski K, Streszewski B, Jaworski W, Luty-Błocho M, Fitzner K. Gold nanoparticles formation via gold(III) chloride complex ions reduction with glucose in the batch and in the flow microreactor systems. Colloids Surf A: Physicochemical Eng Asp 2012;413:208–15.
[58] Watanabe K, Orimoto Y, Nagano K, Yamashita K, Uehara M, Nakamura H, et al. Microreactor combinatorial system for nanoparticle synthesis with multiple parameters. Chem Eng Sci 2012;75:292–7.
[59] Baumgard J, Vogt AM, Kragl U, Jähnisch K, Steinfeldt N. Application of microstructured devices for continuous synthesis of tailored platinum nanoparticles. Chem Eng J 2013;227:137–44.
[60] He Z, Li Y, Zhang Q, Wang H. Capillary microchannel-based microreactors with highly durable ZnO/TiO_2 nanorod arrays for rapid, high efficiency and continuous-flow photocatalysis. Appl Catal B: Environ 2010;93:376–82.
[61] Gutierrez L, Gomez L, Irusta S, Arruebo M, Santamaria J. Comparative study of the synthesis of silica nanoparticles in micromixer–microreactor and batch reactor systems. Chem Eng J 2011;171:674–83.
[62] Jain K, Wu C, Atre SV, Jovanovic G, Narayanan V, Kimura S, et al. Synthesis of nanoparticles in high temperature ceramic microreactors: design, fabrication and testing. Int J Appl Ceram Technol 2009;6:410–9.
[63] Shah RK, Shum HC, Rowat AC, Lee D, Agresti JJ, Utada AS, et al. Designer emulsions using microfluidics. Mater Today 2008;11:28.
[64] Okushima S, Nisisako T, Torii T, Higuchi T. Controlled production of monodisperse double emulsions by two-step droplet breakup in microfluidic devices. Langmuir 2004;20:9905–8.
[65] Shah RK, Kim JW, Agresti JJ, Weitz DA, Chu LY. Fabrication of monodisperse thermosensitive microgels and gel capsules in microfluidic devices. Soft Matter 2008;4:2303–9.
[66] Abate AR, Romanowsky MB, Agresti JJ, Weitz DA. Valve-based flow focusing for drop formation. Appl Phys Lett 2009;94:023503.
[67] Chu LY, Utada AS, Shah RK, Kim JW, Weitz DA. Controllable monodisperse multiple emulsions. Angew Chem – Int Ed 2007;46:8970–4.
[68] Kobayashi J, Mori Y, Okamoto K, Akiyama R, Ueno M, Kitamori T, et al. A microfluidic device for conducting gas–liquid–solid hydrogenation reactions. Science 2004;304:1305–8.
[69] Takei G, Kitamori T, Kim HB. Photocatalytic redox-combined synthesis of L-pipecolinic acid with a titania-modified microchannel chip. Catal Commun 2005;6:357–60.
[70] Chen GW, Li SH, Yuan Q. Pd–Zn/Cu–Zn9Al catalysts prepared for methanol oxidation reforming in microchannel reactors. Catal Today 2007;120:63–70.
[71] Abdallah R, Fumey B, Meille V, de Bellefon C. Micro-structured reactors as a tool for chiral modifier screening in gas–liquid–solid asymmetric hydrogenations. Catal Today 2007;125:34–9.
[72] Kolb G, Hessel V, Cominos V, Hofmann C, Lowe H, Nikolaidis G, et al. Selective oxidations in micro-structured catalytic reactors – for gas-phase reactions and specifically for fuel processing for fuel cells. Catal Today 2007;120:2–20.
[73] Jejurkar SY, Mishra DP. A review of recent patents on micro-combustion and applications. Recent Pat Eng 2009;3:194–209.
[74] Zampieri A, Colombo P, Mabande GTP, Selvam T, Schwieger W, Scheffler F. Zeolite coatings on microcellular ceramic foams: a novel route to microreactor and microseparator devices. Adv Mater 2004;16:819–23.
[75] Takahashi R, Sato S, Sodesawa T, Haga Y, Kobayashi K, Watanabe S, et al. Fabrication of microreactor using glass capillary with Cu/SiO_2 layer. Chem Lett 2006;35:1078–9.
[76] Cui X, Yao D, Li H, Yang J, Hu D. Nano-magnetic particles as multifunctional microreactor for deep desulfurization. J Hazard Mater 2012;205–206:17–23.
[77] Lob P, Lowe H, Hessel V. Fluorinations, chlorinations and brominations of organic compounds in micro reactors. J Fluor Chem 2004;125:1677–94.
[78] Mas ND, Gunther A, Schmidt MA, Jensen KF. Microfabricated multiphase reactors for the selective direct fluorination of aromatics. Ind Eng Chem Res 2003;42:698–710.

[79] Jähnisch K, Baerns M, Hessel V, Ehrfeld W, Haverkamp V, Löwe H, et al. Direct fluorination of toluene using elemental fluorine in gas/liquid microreactors. J Fluor Chem 2000;105:117–28.
[80] Herweck T, Hardt S, Hessel V, Lowe H, Hofmann C, Weise F., et al. Microreaction technology-IMRET 5. In: Proceedings of the 5th international conference on microreaction technology, Springer, Berlin; 2001.
[81] Vankayala BK, Loeb P, Hessel V, Menges G, Hofmann C, Metzke D, et al. Scale-up of process intensifying falling film microreactors to pilot production scale. Int J Chem React Eng 2007;5:1542–5.
[82] Krtschil U, Hessel V, Reinhard D, Stark A. Flow chemistry of the Kolbe-Schmitt synthesis from resorcinol: process intensification by alternative solvents, new reagents and advanced reactor engineering. Chem Eng Technol 2009;32:1774–89.
[83] Xie T, Zeng C, Wang C, Zhang L. Preparation of methyl ester sulfonates based on sulfonation in a falling film microreactor from hydrogenated palm oil methyl esters with gaseous SO_3. Ind Eng Chem Res 2013;52:3714–22.
[84] Maurya RA, Park CP, Kim DP. Triple-channel microreactor for biphasic gas–liquid reactions: photosensitized oxygenations. Beilstein J Org Chem 2011;7:1158–63.
[85] Neuenschwander U, Jensen KF. Olefin autoxidation in flow. Ind Eng Chem Res 2014;53:601–8.
[86] Joshi N, Lawal A. Hydrodeoxygenation of acetic acid in a microreactor. Chem Eng Sci 2012;84:761–71.
[87] Kim SJ, Lee J, Kong KY, Ryul Jung C, Min IG, Lee SY, et al. Hydrogen generation from sodium borohydride using microreactor for micro fuel cells. J Power Sources 2007;170:412–8.
[88] Aran HC, Chinthaginjala JK, Groote R, Roelofs T, Lefferts L, Wessling M, et al. Porous ceramic mesoreactors: a new approach for gas–liquid contacting in multiphase microreaction technology. Chem Eng J 2011;169:239–46.
[89] Inoue T, Kikutani Y, Hamakawa S, Mawatari K, Mizukami F, Kitamori T. Reactor design optimization for direct synthesis of hydrogen peroxide. Chem Eng J 2010;160:909–14.
[90] Rebrov EV, Duisters T, Lovb P, Meuldijk J, Hessel V. Enhancement of the liquid-side mass transfer in a falling film catalytic microreactor by in-channel mixing structures. Ind Eng Chem Res 2012;51:8719–25.
[91] Vanoye L, Aloui A, Pablos M, Philippe R, Percheron A, Favre-Reguillon A, et al. A safe and efficient flow oxidation of aldehydes with O_2. Org Lett 2013;15:5978–81.
[92] Park CP, Kim DP. Dual-channel microreactor for gas – liquid syntheses. J Am Chem Soc 2010;132:10102–6.
[93] Markowz G, Schirrmeister S, Albrecht J, Becker F, Schutte R, Caspary KJ, et al. Microstructured reactors for heterogeneously catalyzed gas-phase reactions on an industrial scale. Chem Eng Technol 2005;28:459–64.
[94] Yube K, Mae K. Efficient oxidation of aromatics with peroxides under severe conditions using a microreaction system. Chem Eng Technol 2005;28:331–6.
[95] Suga S, Nagaki A, Yoshida JI. Highly selective Friedel-Crafts monoalkylation using micromixing. Chem Commun 2003:354–5.
[96] Lowe H, Hessel V, Lob P, Hubbard S. Addition of secondary amines to alpha, beta-unsaturated carbonyl compounds and nitriles by using microstructured reactors. Org Process Res Dev 2006;10:1144–52.
[97] Yao X, Zeng C, Wang C, Zhang L. Two-step continuous synthesis of tetraethylthiuram disulfide in microstructured reactors. Korean J Chem Eng 2011;28:723–30.
[98] Kulkarni AA, Zeyer K-P, Jacobs T, Kienle A. Miniaturized systems for homogeneously and heterogeneously catalyzed liquid-phase esterification reaction. Ind Eng Chem Res 2007;46:5271–7.
[99] Hessel V, Hofmann C, Lob P, Lohndorf J, Lowe H, Ziogas A. Aqueous Kolbe – Schmitt synthesis using resorcinol in a microreactor laboratory rig under high-p,T conditions. Org Process Res Dev 2005;9:479–89.
[100] Zuidhof NT, Croon MHJMD, Schouten JC, Tinge JT. Beckmann rearrangement of cyclohexanone oxime to ε-caprolactam in a microreactor. Chem Eng Technol 2012;35:1257–61.
[101] Wu W, Qian G, Zhou XG, Yuan WK. Peroxidization of methyl ethyl ketone in a microchannel reactor. Chem Eng Sci 2007;62:5127–32.
[102] Wen Z, Yu X, Tu ST, Yan J, Dahlquist E. Intensification of biodiesel synthesis using zigzag micro-channel reactors. Bioresour Technol 2009;100:3054–60.
[103] Sun Y, Sun J, Yao JF, Zhang LX, Xu N. Continuous production of biodiesel from high acid value oils in microstructured reactor by acid–catalyzed reactions. Chem Eng J 2010;62:364–70.
[104] Yao XJ, Yao JF, Zhang LX, Xu NP. Fast esterification of acetic acid with short chain alcohols in microchannel reactor. Catal Lett 2009;132:147–52.
[105] Fukuyama T, Shinmen M, Nishitani S, Sato M, Ryu I. A copper-free Sonogashira coupling reaction in ionic liquids and its application to a microflow system for efficient catalyst recycling. Org Lett 2002;4:1691–4.
[106] Takizawa E, Nagaki A, Yoshida JI. Flow microreactor synthesis of tricyclic sulfonamides via N-tosylaziridinyllithiums. Tetrahedron Lett 2012;53:1397–400.
[107] Ungersboeck J, Philippe C, Haeusler D, Mitterhauser M, Lanzenberger R, Dudczak R, et al. Optimization of [11C]DASB-synthesis: vessel-based and flow-through microreactor methods. Appl Radiat Isot 2012;70:2615–20.
[108] Voros A, Baan Z, Mizsey P, Finta Z. Formation of aromatic amidoximes with hydroxylamine using microreactor technology. Org Process Res Dev 2012;16:1717–26.
[109] Denccicc I, Vaan SD, Noel T, Meuldijk J, Croon MD, Hessel V, et al. Process in a packed-bed microreactor. Ind Eng Chem Res 2013;52:10951–60.
[110] Verma MKS, Ganneboyina SR, Vinayak RR, Ghatak A. Three-dimensional multihelical microfluidic mixers for rapid mixing of liquids. Langmuir 2008;24:2248–51.
[111] Ehrfeld W, Golbig K, Hessel V, Loewe H, Richter T. Characterization of mixing in micromixers by a test reaction: single mixing units and mixer arrays. Ind Eng Chem Res 1999;38:1075–82.
[112] Hardt S, Schonfeld F. Laminar mixing in different interdigital micromixers: II. Numerical simulations. Aiche J 2003;49:578–84.
[113] Liu ZD, Lu YC, Wang JW, Luo GS. Mixing characterization and scaling-up analysis of asymmetrical T-shaped micromixer: experiment and CFD simulation. Chem Eng J 2012;181–182:597–606.
[114] Rosenfeld C, Serra C, Brochon C, Hessel V, Hadziioannou G. Use of micromixers to control the molecular weight distribution in continuous two-stage nitroxide-mediated copolymerizations. Chem Eng J 2008;135:S242–6.
[115] Iwasaki T, Kawano N, Yoshida J. Radical polymerization using microflow system: numbering-up of microreactors and continuous operation. Org Process Res Dev 2006;10:1126–31.
[116] Nisisako T, Torii T, Higuchi T. Novel microreactors for functional polymer beads. Chem Eng J 2004;101:23–9.
[117] Wu T, Mei Y, Cabral JT, Xu C, Beers KL. A new synthetic method for controlled polymerization using a microfluidic system. J Am Chem Soc 2004;126:9880–1.
[118] Wu T, Mei Y, Xu C, Byrd HCM, Beers KL. Block copolymer PEO-b-PHPMA synthesis using controlled radical polymerization on a chip. J Micromechnical Microengineering 2004;14:153.
[119] Iwasaki T, Yoshida J. Free radical polymerization in microreactors. Significant improvement in molecular weight distribution control. Macromolecules 2005;38:1159–63.
[120] Rosenfeld C, Serra C, Brochon C, Hadziioannou G. Influence of micromixer characteristics on polydispersity index of block copolymers synthesized in continuous flow microreactors. Lab Chip 2008;8:1682–7.
[121] Matthias C, Thomas J. Fast and efficient [2+2] UV cycloaddition for polymer modification via flow synthesis. Macromolecules. Unpublished results.
[122] Wurm F, Wilms D, Klos J, Lowe H, Frey H. Carbanions on tap-living anionic polymerization in a microstructured reactor. Macromol Chem Phys 2008;209:1106–14.
[123] Iida K, Chastek TQ, Beers KL, Cavicchi KA, Chun J, Fasolka MJ. Living anionic polymerization using a microfluidic reactor. Lab Chip 2009;9:339–45.
[124] Yasuhiro U, Yoichi MAY, Tomohiko B, Naoshi F, Masaharu U, Takehiko K. Instantaneous carbon-carbon bond formation using a microchannel reactor with a catalytic membrane. J Am Chem Soc 2006;128:15994–5.
[125] Bhangale AS, Beers KL, Gross RA. Enzyme-catalyzed polymerization of end-functionalized polymers in a microreactor. Macromolecules 2012;45:7000–8.
[126] Lewis PC, Graham RR, Nie ZH, Xu SQ, Seo M, Kumacheva E. Continuous synthesis of copolymer particles in microfluidic reactors. Macromolecules 2005;38:4536–8.
[127] Dubinsky S, Zhang H, Nie Z, Gourevich I, Voicu D, Deetz M, et al. Microfluidic synthesis of macroporous copolymer particles. Macromolecules 2008;41:3555–61.
[128] Nagaki A, Miyazaki A, Yoshida JI. Synthesis of polystyrenes-poly(alkyl methacrylates) block copolymers via anionic polymerization using an integrated flow microreactor system. Macromolecules 2010;43:8424–9.
[129] Honda T, Miyazaki M, Nakamura H, Maeda H. Controllable polymerization of N-carboxy anhydrides in a microreaction system. Lab Chip 2005;5:812–8.
[130] Kessler D, Lowe H, Theato P. Synthesis of defined poly(silsesquioxane)s: fast polycondensation of trialkoxysilanes in a continuous-flow microreactor. Macromol Chem Phys 2009;210:807–13.
[131] Huang KS, Lai TH, Lin YC. Manipulating the generation of Ca-alginate microspheres using microfluidic channels as a carrier of gold nanoparticles. Lab Chip 2006;6:954–7.
[132] Liu K, Ding HJ, Liu J, Chen Y, Zhao XZ. Shape-controlled production of biodegradable calcium alginate gel microparticles using a novel microfluidic device. Langmuir 2006;22:9453–7.
[133] Wang T, Oehrlein S, Somoza MM, Sanchez Perez JR, Kershner R, Cerrina F. Optical tweezers directed one-bead one-sequence synthesis of oligonucleotides. Lab Chip 2011;11:1629–37.
[134] Peterson DS, Rohr T, Svec F, Frechet JMJ. Enzymatic microreactor-on-a-chip: protein mapping using trypsin immobilized on porous polymer monoliths molded in channels of microfluidic devices. Anal Chem 2002;74:4081–8.
[135] Khoo HS, Lin C, Huang SH, Tseng FG. Self-assembly in micro- and nanofluidic devices: a review of recent efforts. Micromachines 2011;2:17–48.
[136] Dendukuri D, Doyle PS. The synthesis and assembly of polymeric microparticles using microfluidics. Adv Mater 2009;21:4071–86.
[137] Chein RY, Chen LC, Chen YC, Chung JN. Heat transfer effects on the methanol-steam reforming with partially filled catalyst layers. Int J Hydrogen Energy 2009;34:5398–408.
[138] Lopez-Orozco S, Inayat A, Schwab A, Selvam T, Schwieger W. Zeolitic materials with hierarchical porous structures. Adv Mater 2011;23:2602–15.